Interactions between mechanisms of reproductive isolation

Alexandre Blanckaert[a*] and Vitor C. Sousa[a]

[a] cE3c - Centre for Ecology, Evolution and Environmental Changes & CHANGE - Global Change and Sustainability Institute, Faculdade de Ciências, Universidade de Lisboa, Campo Grande, Portugal

Corresponding author *: blanckaert.a@gmail.com

Conflict of interest: The authors declare no conflict of interest.

Funding: This work was funded by the strategic project UIDB/00329/2020 granted to CE3C from the Portuguese National Science Foundation Fundação para a Ciência e a Tecnologia (FCT). This study was funded by HFSP Young Investigator Grant RGY0081/2020 to V.S., FCT Grant 2022.03475.PTDC to A.B. and V.S. and FCT Grant DOFLOW to V.S.. We thank the National Network for Advanced Computing (RNCA) and INCD (incd.pt) for access and use of their computing infrastructure, funded by FCT to A.B. and V.S. (2022.38032.CPCA.A0 and 2022.15858.CPCA.A2).

Author contributions: A.B. and V.S. designed the study, A.B. wrote the simulation code and conducted the analysis, and A.B. and V.S. wrote the manuscript.

Acknowledgments: We thank João Carvalho, Inês Fragata and the Evolutionary Genomics and Bioinformatics lab for discussion of the project and Claudia Bank for comments on the manuscript.

Abstract

Speciation is responsible for the diversity of species observed today and corresponds to the build-up of reproductive isolation between populations. Reproductive isolation can be generated by different mechanisms that have been extensively characterized, yet how their interactions affect speciation remains largely unknown. Here, we explicitly model the interaction of three key mechanisms (local adaptation, mate choice and genetic hybrid incompatibilities) quantifying their relative contribution to the evolution of reproductive isolation. We modeled two populations exchanging migrants using Fisher's Geometric Model for local adaptation, phenotype matching for mate choice, and multiple pairs of Bateson-Dobzhansky-Muller Incompatibilities (DMI). All three mechanisms were determined by the same set of loci, creating conditions for interactions between barriers both at the genetic and population levels. We found very few cases where the three barriers evolved together. Instead, two barriers could evolve depending on the migration rate: either local adaptation and genetic incompatibilities for limited migration, or local adaptation and mate choice for higher migration. Our results showed that local adaptation due to ecological differentiation was the first to evolve and by far the most effective reproductive barrier. Finally, we demonstrated that in a polygenic model, populations could become locally adapted and evolve strict mate choice, yet they would not accumulate incompatibilities provided that there was sufficient gene flow.

Speciation has been a central theme in evolutionary biology since its early origin (Darwin, 1859). Yet, despite a truly large body of work (Kirkpatrick and Ravigné, 2002), general rules of how speciation works and which mechanisms are involved remain to a large extent a mystery. So far, most findings provide a case by case set of rules rather than universal ones (see Table 1 in Sobel et al., 2010). Two key questions have been under active research and debate. First, what should be measured to capture progress in the speciation process (Westram et al., 2022; Mallet and Mullen, 2022)? Second, what is the end of the speciation process? This was historically defined as complete reproductive isolation (RI) between the two diverging populations (Coyne and Orr, 2004). However, recent advances in genomics reveal that gene flow between well-defined species is far from uncommon (Payseur and Rieseberg, 2016), making it difficult to draw the line of when speciation completes (Hey and Pinho, 2012; Dopman et al., 2024). Furthermore, it has been recently argued that partial RI may not be a transient state on the way to speciation but that it may also be "a final equilibrium" state (Servedio and Hermisson, 2020; Barraclough, 2024) further blurring the notion of species.

Different mechanisms of RI can drive the speciation process. They have been classified depending on the timing (pre- or postzygotic) and nature of selection acting upon the mechanism of RI (extrinsic or intrinsic) (Coyne and Orr, 2004). Disentangling which RI mechanism(es) have the largest impact during speciation, and whether their interactions are synergistic or antagonistic remained a central question of speciation research. In other words, do we observe coupling ("coincidences of barrier effects, resulting in a stronger overall barrier to gene flow", sensu Butlin and Smadja, 2018, synergistic interactions) or a diminution of the overall strength of the RI barrier (antagonistic)? There have been many attempts to characterize the joint evolution of different mechanisms of RI (e.g., mate choice, hybrid load), or the evolution of one conditioned on the other, with assortative mating models via "magic trait" or reinforcement being the more widely known examples.

Indeed, the coupling of RI barriers is considered an important step in the speciation process (Barton, 1983; Butlin and Smadja, 2018; Dopman et al., 2024). Yet, it may lead to overall weaker rather than stronger RI (Aubier et al., 2024), and it remains unclear under which conditions multiple barriers lead to synergistic or antagonistic outcomes. Theoretical studies have shown that multiple RI barriers do not always act synergistically. For instance, Maisonneuve et al. (2024) investigated the case where mate choice could evolve to use either a cue under positive selection in both populations or a neutral one. The authors showed that, rather than coupling mate choice with the trait under positive selection, the neutral cue was favored over the cue affecting fitness, when the risk of choosing the wrong mate was too high (and F_1s were unviable).

There has been a recent push to fully characterize the different RI barrier acting between pairs of nascent species. For example, male mate choice and (almost complete) hybrid sterility have been reported between *Tetranychus cinnabarinnus* and *T. urticae* spider mites (Cruz et al., 2024). In addition, *T. urticae* adaptation to host plants has been shown to have a polygenic basis (Villacis-Perez et al., 2024). Similarly, in natural populations of *Xiphophorus birchmanni* and *X. malinche* swordtail fish, strong assortative mating (female choice) and (some level of) hybrid dysfunction has been identified in artificial crosses (Aguillon et al., 2025). In the later case, genetic incompatibilities have been identified between mitochondrial proteins, likely associated with thermal adaptation. Indeed, the same two swordtail fish species are adapted to different thermal environments and their hybrids display "widespread misregulation" of thermotolerance genes, suggesting an overlap between genes under local adaptation and the one responsible for genetic incompatibilities (Payne et al., 2024). However, quantifying the role of these mechanisms in natural populations can be challenging, even for species amenable to laboratory manipulation (e.g., Aguillon et al., 2025). In addition, there are no general rules emerging. For example, Castillo et al. (2015) conducted experimental evolution of *Caenorhabditis remanei* on different substrates, measuring the evolution of local adaptation, mate choice and genetic incompatibilities, concluding that local adaptation was not relevant for the evolution of RI. This contrasts with other studies highlighting the importance of local adaptation in natural populations (reviewed in Rundle and Nosil, 2005, Table 1), with many empirical examples of ecological speciation: Darwin finches (Grant and Grant, 2024), ciclids (McGee et al., 2020), freshwater stickleback (Hatfield and Schluter, 1999; Marques et al., 2019), whitefish (Rogers and Bernatchez, 2007) *Heliconius* butterfly (Mallet and Barton, 1989), and pea aphids (Via et al., 2000).

While the spatial context of speciation (i.e., allopatric, parapatric and sympatric) has historically been strongly debated, several authors proposed to consider whether speciation occurs with or without gene flow, irrespective of the spatial context (Butlin et al., 2008; Stankowski and Ravinet, 2021; Bolnick et al., 2023). When there is gene flow between populations (non sterile F_1s), genetic incompatibilities create a hybrid load that may act as a sieve, leading to removal of genetic incompatibilities from both populations. Thus, provided that the mutations involved in incompatibilities do not confer local selective advantage, or are not tightly linked to a mutation that does, we expect genetic incompatibilities to be lost when there is gene flow (Agrawal et al., 2011; Bank et al.,

2012; Blanckaert and Hermisson, 2018). In addition, migration between two populations in contact with each other creates divergent selection on mate choice traits (McPeek and Gavrilets, 2006; Yamaguchi and Iwasa, 2013) to avoid the production of unfit hybrids (whether the cause is intrinsic or extrinsic). Overall, this makes migration and the strength of gene flow a key parameter to any study relative to speciation.

Here, we characterized how local adaptation, mate choice and genetic incompatibilities interact with each other, quantifying their impact on the strength of RI between two populations evolving with migration. We investigated whether the evolution of one mechanism impacts the evolution of the others, and quantified their interaction by assessing their joint effect on RI, compared to their individual contributions. We focus on three specific mechanisms of RI, each standing for a different type according to the classification mentioned above: mate choice (here an intrinsic prezygotic mechanism), accumulation of genetic incompatibilities (intrinsic postzygotic) and local adaptation (extrinsic pre- and postzygotic). In particular, we designed a model where RI mechanisms interact with each other at the genetic level: a large number of loci contribute to the phenotype of the individual, allowing for a polygenic basis for adaptation (Mackay, 2001), with a subset forming intrinsic genetic incompatibilities. Multiple authors have argued that such shared genetic basis should be common (Schluter and Conte, 2009; Kulmuni and Westram, 2017), with some empirical evidences identified in *Mimulus guttatus* (copper tolerance, Macnair and Christie, 1983) or *Arabidopsis thaliana* (resistance against biotrophic pathogens, Świadek et al., 2017). Recently, Frayer et al. (2025) compiled a list of known genetic incompatibilities - among them the most likely explanation for 18% of DMIs was host pathogen conflicts and adaptation for 4.2%. Moreover, the fitness of an individual is defined as the compound effect of extrinsic and intrinsic fitness; the first term is determined by the phenotype (i.e., how well adapted it is to the environment) and the second by the intrinsic genetic load due to genetic incompatibilities. Finally, (intrinsic) mate choice is based on the phenotype distance between potential mates (phenotype matching). This last assumption corresponds to a "classical magic trait" (according to the classification of Servedio et al., 2011) and has been reported in various organisms: wing pattern in *Heliconius* butterfly (Mallet and Barton, 1989; Jiggins et al., 2001, 2005) or body size in stickleback fishes (Snyder and Dingle, 1989; McKinnon et al., 2004); for a more complete list of biological putative examples, see Table 1 of Servedio et al. (2011). As argued by Thibert-Plante and Gavrilets (2013), these traits might be more common than expected, as selection favors their formation when initially absent. Under this model, we showed that local adaptation was the first mechanism to evolve and also the key mechanism responsible for the strength of reproductive isolation. Typically, depending on the level of migration between populations, either mate choice or the accumulation of genetic incompatibilities evolved in tandem with local adaptation. Interestingly, we found that even populations that evolve local adaptation and strict mate choice, might not accumulate genetic incompatibilities, provided that there was sufficient gene flow.

Model

Population model

To understand the effect of a common underlying genetic architecture for the three reproductive isolation (RI) barriers, an hypothesis that should favor the joint evolution of RI barriers, we investigated a polygenic model where loci determining the phenotype, which affected local adaptation and mate choice, could also be involved in genetic incompatibilities, as illustrated in Figure 1. Due to the complex polygenic genetic basis of the phenotype and genetic incompatibilities, we used individual-based simulations to investigate the long term evolution ($> 10N$ generations) of two populations of N diploid dioecious individuals (per default, $N = 10,000$) exchanging migrants at rate m (two-island-island model; per default $m = 0.05$). To model local adaptation, we considered that the two islands represent two environments (A and B) with different phenotypic optima, and for simplicity, we referred to the population residing in each environment as population A and B, respectively. We let the phenotype, genetic incompatibilities and mate choice evolve, exploring the impact of key processes in the build-up of RI. As detailed below, we varied: (1) the extent of migration ($0.0 \leq m \leq 0.2$), (2) the genetic architecture of phenotypes and intrinsic genetic incompatibilities, (3) life history of species (juvenile vs adult dispersal stage), and (4) initial levels of divergence between populations (ancestral vs secondary contact), keeping the other parameters fixed (see Table 1 for the complete list of parameters).

We considered that the overall fitness of an individual (before mate choice) resulted from the combined effects of intrinsic and extrinsic fitness components. The extrinsic fitness depended on the phenotype of a given individual and its environment. Importantly, a subset of the loci that coded the phenotype (i.e., involved in local adaptation) also formed pairs of genetic incompatibilities, determining the intrinsic fitness. Mate choice was modeled as assortative mating (in its stricter sense, i.e., positive assortative mating, Jiang et al., 2013), with individuals preferring mates with phenotypes similar to their own, depending on the genotype at a single modifier locus and a (fixed) cost associated to choosiness. Finally, we compared the results of models with a common genetic architecture to instances where the different barriers did not share a common genetic basis (see Starting conditions section).

The life cycle of individuals from both populations included the following sequence of events at each generation: (i) selection (based on intrinsic and extrinsic fitness components), (ii) migration, (iii) mating and (iv) zygote formation (including recombination and mutation). We considered two possible life cycles differing in whether selection or migration occurred first, i.e., differing in the dispersal stage of the organism. With "adult dispersal", selection occurred before migration, whereas with "juvenile dispersal" selection occurred after migration. Since fitness of an individual was computed when it reached adulthood, the difference between the two life cycles was caused by the dispersal stage and whether immigrating individuals had their fitness determined by the environment they were born in ("adult dispersal") or by the environment they inhabited at the time

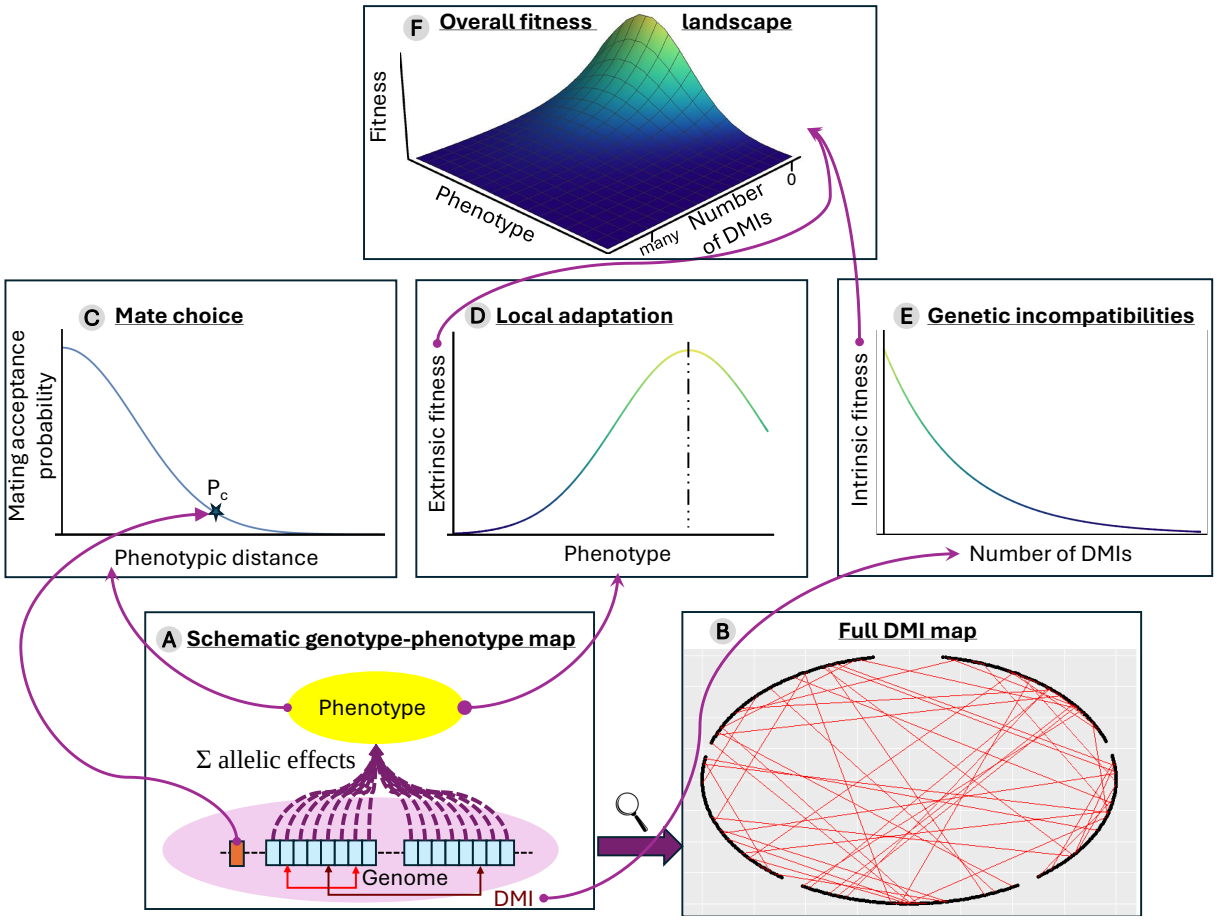

Figure 1: Schematic illustration of the genetic basis of the different mechanisms of reproductive isolation (RI). The diploid genome (panel A) consists of L loci separated in n_{LB} linkage blocks depicted by the blue squares. Their effect on each phenotypic trait are summed to generated the phenotype, depicted in yellow. In addition, a modifier locus (in dark orange) controls the strength of choosiness (P_C), which determines how steep the probability of accepting a mating is (panel C, see eq. (3)). The phenotype determines the extrinsic fitness through a quadratic function (panel D, see eq. (1)). Finally, genetic incompatibilities are depicted by the red arrows between blue squares (panel B for the full map for the "default" scenario), and their number determined the intrinsic fitness (panel E, see eq. (2)). The overall fitness (before mate choice) is obtained by combining extrinsic and intrinsic fitnesses, as depicted in panel F.

of reproduction ("juvenile dispersal").

Migration was modeled as a Poisson process, of parameter $N \times m$. Population size N was assumed to be the same in both populations and constant when forming the next generation. Each population, regardless of the number of adults, produced N offspring with a 50:50 sex ratio.

Genotype and phenotype: The genome of each diploid individual was composed of two different (autosomal) elements: a modifier locus determining mate choice and one large genomic element determining the phenotype and genetic incompatibilities, composed of L biallelic loci (per default, $L = 500$) distributed equally over n_{LB} linkage blocks (fixed to $n_{LB} = 5$). These L biallelic loci determined the n_t quantitative traits (per default, $n_t = 1$). Mutation was bidirectional, symmetric and happened at rate μ (per default, $\mu = 10^{-6}$ per generation per locus). All mutations were pleiotropic and isotropic

(affecting all n_t phenotypic traits equally), with phenotypic effects $(z_{i1}, .., z_{in_t})$ for the n_t traits drawn from a multivariate centered normal distribution with the covariance matrix $\Sigma = \sigma_\mu^2 I_{n_t}$, where I_{n_t} is the identity matrix and σ_μ^2 the variance of mutational effects (fixed to $\sigma_\mu = 0.05$). Mutational effects were additive at the phenotypic level, hence the phenotype of a (diploid) individual was given by $Z_j = \sum_{i=1}^{L} X_i z_{ij}$, for a given phenotypic trait j, with X_i taking the value 0 if the individual was homozygous for ancestral allele, 1 if heterozygous and 2 if homozygous for the derived allele at locus i. For simplicity, we will refer to the phenotype that is at the optimum in the focal environment as the "optimal phenotype", and to the phenotype at the optimum in the other environment as the "alternative phenotype". Given that we only explored a low number of phenotypic traits (1 to 3), we did not correct the mutational effect size by the size of the phenotypic space. Recombination between adjacent loci (within a block) happened at rate ρ (fixed to $\rho = 10^{-3}$ per individual and per generation), while recombination between linkage blocks happened at rate ρ_{LB} (fixed to $\rho_{LB} = 10^{-2}$).

For mate choice, we modeled choosiness as a single modifier locus (Haldane, 1941; Nei, 1967; Feldman et al., 1996) with multiple alleles, rather than a quantitative trait with many underlying loci. Mutation happened at a fixed rate 10μ at the choosiness locus and the new allele differed from the current allelic value by a deviation drawn from a normal centered distribution with variance σ_p^2 (fixed to $\sigma_p = \sigma_\mu = 0.05$). The effect of alleles was additive and allelic values exceeding the boundaries (< 0 or > 0.5) upon mutations were set to the corresponding boundary value. The choosiness locus was situated at the beginning of the main genomic element, at a genetic distance ρ_{MC} from the first position of the first linkage block (fixed to $\rho_{MC} = 0.1$).

Given that the range of values that the phenotype and mate choice could take was bounded, these traits suffered from a mutational bias: when the phenotypic trait (or the mate choice allele effect) reached values close to their extrema, the mean displacement caused by new mutations was, on average, no longer 0 but biased towards the other extremum (Fig. S1). Thus, mutational bias acts against divergence of populations and evolution of strict mate choice. This differs from other theoretical studies where mutation bias, in a male display trait, promoted the evolution of choosiness in females (Pomiankowski et al., 1991; Andersson and Iwasa, 1996).

Sex was not genetically determined, and was randomly assigned to each individual at birth according to the expected sex ratio (50:50).

Fitness: The fitness w of an individual before mate choice was obtained by considering both extrinsic w_{ext}^A (due to the environment, here A) and intrinsic (due to the genetic incompatibilities) w_{int} components: $w = w_{ext}^A \times w_{int}$, and corresponded to the relative probability of an individual to initiate a mating. Note that initiating a mating did not imply reproduction, since choosiness and cost of choosiness could impact the outcome.

Local adaptation (extrinsic fitness): The extrinsic component of fitness was modeled using Fisher's Geometric Model (Fisher, 1930). Indeed, this model accurately captured the distribution of fitness effect of mutations across different organisms (e.g., vesicular stomatitis virus, *Escherichia coli*, *Drosophila melanogaster* or *Triticum durum*, Martin and Lenormand, 2006) or *Arabidopsis thaliana* (Stearns and Fenster, 2016). The

(absolute) fitness of each individual depended on the (Euclidean) distance between their phenotype, given by the $(Z_1, .., Z_{n_t})$ vector over the n_t phenotypic traits, and the environmental optimum. The relation between phenotype and fitness was obtained from Gros et al. (2009) with a slightly different choice of parametrization, to explicitly account for fitness in the alternative environment (see Appendix). The fitness of an individual in environment A was given by:

$$w_{ext}^{A} = e^{log(\Omega^B)\left(\frac{\Sigma_{j=1}^{n_t}(Z_j - Z_j^A)^2}{\Delta_{AB}}\right)^{\frac{Q}{2}}} \tag{1}$$

where Z_j is the phenotypic value of trait j, Z_j^A is the optimal phenotypic value for trait j in environment A, Δ_{AB} is a constant corresponding to the squared (Euclidean) distance between the phenotype of two individuals at the optima in environment A and environment B ($\Delta_{AB} = \Sigma_{j=1}^{n_t}(Z_j^A - Z_j^B)^2$; per default, $\Delta_{AB} = 100$), Q controls the shape of the landscape ($Q \in [0, \infty[$; per default, $Q = 2$), and Ω^B is a constant corresponding to the fitness of an individual in environment A with a phenotype perfectly adapted to environment B (i.e., $Z_j = Z_j^B$). In this fitness landscape (Gros et al., 2009) when $Q < 2$, epistasis between pairs of mutations at the optimum was positive on average, otherwise it was negative (with null epistasis for $Q = 2$). The fitness in environment B (w_{ext}^B) was obtained by substituting Z_j^A by Z_j^B, and Ω^B by Ω^A (per default, $\Omega^A = \Omega^B = 0.1$). The shape of the landscape determined the fitness of the F_1 individuals with regards to the parents (see Appendix and equation (A3)). Under the default parameters (Table 1), weak hybrid vigor was the default behavior.

Genetic incompatibilities (Intrinsic fitness): We modeled intrinsic fitness, as pairs of Bateson-Dobzhansky-Muller incompatibilities (DMIs, Bateson, 1909; Dobzhansky, 1936; Muller, 1942). Importantly, as mentioned above, the loci involved in incompatibilities also affected the phenotype and therefore could be involved in local adaptation. We considered n_{DMI} pairs of incompatibilities (per default, $n_{\text{DMI}} = 50$), with the loci chosen among the L loci that affected the individual phenotype. Per default, each locus could form at most a single DMI (sampling without replacement), with the two interacting loci chosen independently of their position along the genome. Each DMI was codominant and their interaction multiplicative, resulting in the following formula for the intrinsic fitness component:

$$w_{int} = \Pi_{k=1}^{n_{\text{DMI}}}(1 - \epsilon^{X_k Y_k}) \tag{2}$$

where X_k and Y_j are the counts of the number of derived alleles (0, 1 or 2) at the two loci forming the DMI, and ϵ is the strength of epistasis (i.e, the reduction in fitness due to a single DMI; per default, $\epsilon = 0.1$). As extensions, we explored some of the hypotheses formulated above, detailed in the "Starting conditions" section.

Mate choice: We modeled mate choice using a phenotype matching approach following Irwin (2020), where the probability of accepting a mate depended on the phenotypic distance between the two individuals, and was given by a Gaussian function. Rather than defining a variance, the shape of the Gaussian function was controlled by one parameter,

P_C (Fig. S2), that corresponded to the probability of an individual with the "optimal phenotype" accepting a mate with the "alternative phenotype" (see Appendix). Motivated by the spider mite example, we assumed that males were the choosy individuals. While mate choice has often been modeled as female choice (e.g., Servedio and Boughman, 2017) and male choice is rarer and possible under stricter conditions (Fitzpatrick and Servedio, 2018), it is still frequently found in nature (reviewed in Barry and Kokko, 2010). Regardless, the results held true for female choice too, as no aspect of mate choice was sex-specific in our model and both males and females can mate multiple times. Mate choice proceeded as followed: a male and χ potential females (sampling with replacement) were chosen (fixed to $\chi = 100$), according to their respective fitness. Second, the male considered mating with the first potential female, accepting said mating according to his choosiness (P_C) and how phenotypically similar the two potential mates were, with probability

$$P(mating) = \begin{cases} 1 & \text{if } P_C = 0 \text{ and } \Sigma_{j=1}^{n_t}(Z_j^m - Z_j^f)^2 = 0 \\ e^{log(P_C)\frac{\Sigma_{j=1}^{n_t}(Z_j^m - Z_j^f)^2}{\Delta_{AB}}} & \text{otherwise} \end{cases} \tag{3}$$

where Z_j^m and Z_j^f are the phenotypes at trait j of males and females, respectively. If the mating was accepted, a single offspring was produced and a new set of one male and χ females were selected. If the first potential female was rejected, the male would be considered for mating with the second female. This process continued until a mating was accepted or all χ females were rejected. If a male failed to accept any of the χ potential females, the male was discarded (but available to be chosen to initiate a mating again based on his fitness). This process continued until N offspring were produced. The number of potential females considered by a male for a mating (χ) therefore corresponds to a cost of choosiness, ranging from costly ($\chi = 1$) to cost-free ($\chi \to \infty$). As mentioned above, choosiness (P_C) was determined genetically by the modifier locus, with values varying between 0 (strict assortative mating) and 1 (no choosiness) at the phenotypic level, and therefore between 0 and 0.5 at the allelic level.

Starting conditions and population metrics: We let RI barriers evolve for $50N$ generations, considering three possible starting conditions:

- "Ancestral" state: both populations started identical and were fixed for allele 0 at all biallelic loci. There was no initial assortative mating ($P_C = 1$).
- Secondary contact state, "SC": the two populations started with alleles differently fixed for each DMI locus, and at all remaining biallelic L loci affecting the phenotype alleles took values such that individuals from each environment were close to their optimum (i.e., for each phenotypic trait j, $Z_j \approx Z_i^A$ for environment A and $Z_j \approx Z_i^B$ for environment B). There was no initial assortative mating ($P_C = 1$).
- Secondary contact with initial mate choice state, "SC + initial mate choice": the starting conditions were identical to the "SC" state but with preexisting strict mate choice ($P_C = 10^{-4}$).

Regardless of the starting conditions, populations were always in a monomorphic state at the start of the simulations (i.e., all individuals were identical in each population).

We kept track of the population by computing the mean absolute fitness, as well as its extrinsic and intrinsic components, the mean phenotype, the mean choosiness and the hybrid load between populations (defined below). All metrics were computed, per population, for adult individuals after selection and migration had already occurred. In particular, this meant that if all individuals of the two populations were at the phenotypic optimum at A (Z_j^A) and B (Z_j^B), the mean phenotype for trait j of population A depended on migration and was given by $\bar{Z}_j = (1-m)Z_j^A + mZ_j^B$.

The hybrid load was defined as the reduction in (intrinsic) fitness caused by genetic incompatibilities. This was quantified by computing the intrinsic fitness component of simulated ephemeral (not part of the next generation) F_1 individuals resulting from the cross of individuals from the two populations, correcting by the mean intrinsic fitness to their parents ($\bar{w}_{int}^A$ and $\bar{w}_{int}^B$). This correction allows us to disentangle the hybrid load (defined as the reduction in fitness due to genetic incompatibilities present in different populations) from the mutational load caused by DMIs segregating within each population. The ephemeral F_1 individuals were obtained with males of population A (resp. B) choosing females of population B (resp. A), according to their choosiness. We focused on ephemeral F_1 individuals since all DMIs between populations would be in the double heterozygote state. Therefore, we could compute the number of equivalent fixed DMIs needed to generate the observed hybrid load (corrected by within population mutational load due to genetic incompatibilities):

$$n_{\mathrm{DMI}}^{eq} = \frac{1}{log(1-\epsilon)} \times log\left(\frac{2\bar{w}_{F_1}^{int}}{\bar{w}_{int}^A + \bar{w}_{int}^B}\right) \tag{4}$$

where $\bar{w}_{F_1}^{int}$ is the mean intrinsic fitness of hybrids, and ϵ is the strength of epistasis due to DMIs. In scenarios with migration, this equivalent number of fixed DMIs could be underestimated since populations would contain a proportion of individuals with the alternative phenotype. Hence, immigrant males, from population A, would prefer to mate with those females, with an environment A phenotype despite their lower extrinsic fitness. Such matings would produce individuals with the environment A phenotype, that were likely DMI-free, regardless of the genetic distance between the A and B population, reducing the generation of F_1s expressing DMIs, and therefore resulting in a lower hybrid load between populations. This effect could be further exacerbated by the dispersal stage, especially with "adult dispersal", when selection preceded migration.

Unless specified otherwise, we used a single genetic background (i.e., map of genetic interaction and mutational effects) for a given set of relevant parameters (i.e., for $\{L, n_t, n_{\mathrm{DMI}}\}$). In particular, we used the following genetic architecture maps:

- "default" map: 50 DMIs pairs (100 loci, $n_{\mathrm{DMI}} = 50$) among the $L = 500$ loci affecting a single phenotypic trait ($n_t = 1$). Each locus could be involved in at most a single DMI pair. This is the map illustrated in Figure 1B.

- "default 3D" map: 50 DMIs pairs (100 loci, $n_{\mathrm{DMI}} = 50$) among the $L = 500$ loci affecting three phenotypic traits ($n_t = 3$). Each locus could be involved in at most a single DMI pair.

- "optimized" map: 250 DMIs pairs (500 loci, $n_{\mathrm{DMI}} = 250$) among $L = 500$ loci affecting a single phenotypic trait ($n_t = 1$). The 250 loci affecting the phenotype positively interacted in a pairwise and unique way with the 250 loci affecting the phenotype negatively. We investigated this map, because, while unrealistic, it minimized the possible genetic conflict between ecological divergence and genetic incompatibilities, and therefore should be more likely to lead to accumulation of DMIs.

- "neutral" map: The genome was formed by $L = 800$ loci: half of them, chosen randomly, affected the phenotype, while the other 400 loci did not and formed 200 pairs of DMIs ($n_{\mathrm{DMI}} = 200$). Each locus was involved in a single DMI pair. The phenotype consisted of a single trait ($n_t = 1$). We investigated this map to separate the loci involved in local adaptation and DMIs.

- "network" map: The genome was formed by $L = 800$ loci: half of them, chosen randomly, affected the phenotype, while 50 loci were randomly picked among the other 400 (neutral) loci and formed 200 DMIs pairs ($n_{\mathrm{DMI}} = 200$). The phenotype consisted of a single trait ($n_t = 1$). We investigated this map to assess whether a network of DMIs promoted the accumulation of DMIs.

- "neutral display" map: 50 DMIs pairs (100 loci, $n_{\mathrm{DMI}} = 50$) among $L = 500$ loci affecting the phenotype, which was defined as two phenotypic traits $n_t = 2$. In this case, the first phenotypic trait affected the extrinsic fitness and the second one was used as cue for mate choice. The mutational effects on the first phenotypic trait and the DMIs pairs were identical to the "default" map.

Following Kirkpatrick and Ravigné (2002) classification, our approach included all five majors elements: with 1) fitness varying in space, 2) assortative mating, 3) a "magic" trait so that direct selection promoting local adaptation also affects the trait used for mate choice, 4) a modifier locus for choosiness, and 5) considering either low ("ancestral") or large ("secondary contact") initial divergence.

Measuring Reproductive Isolation (RI): reduction in gene flow caused by each RI mechanism

Defining and measuring RI between populations remains a debated topic (Westram et al., 2022). Here we followed the definition proposed by Westram et al. (2022) and measured RI as the reduction in gene flow at a neutral marker. Thus, we considered the fate of alleles at two neutral markers, one freely recombining and the other situated in the middle of the genome. One individual (referred to as focal) from the population A was transferred to population B. We followed the fate of the alleles from population A at these two neutral markers, which were introduced with an absolute frequency of two as the focal

individual was homozygous at the two marker loci, over a maximum of N generations. Note that simulations to measure RI were done after the last generation of the long term evolution. For convenience, we refer to this as post-evolution simulations, and its initial starting time as generation 0 post-evolution. The fate of these alleles was always tracked with the two populations in isolation, regardless of the initial migration rate. We chose this design to avoid the neutral marker surviving in the alternative population through back migration. Although invasion probability was the most obvious metric to track, it was computationally heavy, especially when considering large populations. Therefore, we measured the time of loss of the neutral markers or their frequency after N generations post-evolution, if they were still polymorphic. We considered the fate of 1,000 invasion events (each time choosing the focal individual randomly) in populations of $N = 10,000$ individuals.

We measured the strength of RI post-evolution, accounting for the parameter values that evolved at each barrier (i.e., alleles at phenotypic loci, genetic incompatibility loci and male choosiness locus). To assess the relative impact of each mechanism of RI, we simulated the invasion of focal individuals either accounting to the effect of the three barriers, a combination of two barriers, or just one barrier. This was done by turning off barriers, which corresponded to fixing the extrinsic fitness, intrinsic fitness or male choosiness (or any combination of these two) to 1. For instance, to assess the relative impact of of local adaptation, we computed the mean time of loss by only considering the extrinsic fitness values (w^A_{ext} and w^B_{ext} at the two environments, respectively), setting the intrinsic fitness and male choosiness to 1 (i.e., $w_{int} = 1$,$P_C = 1$). Thus, there were eight different possible combinations of mechanisms of RI (referred to as "RI barriers" for the rest of manuscript).

Parameter	Variable	Default value	Status
Population size	N	10,000	Variable
Number of loci	L	500	Variable
Number of linkage blocks	n_{LB}	5	Fixed
Recombination rate between adjacent loci (per individual per generation)	ρ	0.001	Fixed
Recombination rate between linkage block (per individual per generation)	ρ_{LB}	0.01	Fixed
Recombination rate between choosiness locus and first locus (per individual per generation)	ρ_{MC}	0.1	Fixed
Number of phenotypic traits	n_t	1	Variable
Mutation rate (per individual per base pair per generation)	μ	10^{-6}	Fixed
Standard deviation of mutational effects	σ_μ	0.05	Fixed
Standard deviation for mutation at the choosiness loci	σ_P	0.05	Fixed
Standard deviation for mutation at the cost loci	σ_C	0	Fixed
Shape of Fisher's Geometric model controlling the average epistasis	Q	2	Variable
Optimal phenotype at trait j for environment A (and B)	z_j^A (z_j^B)	5 (-5)	Variable
Squared distance between perfectly adapted individuals from environment A and B	Δ_{AB}	100	Variable
Fitness of an optimal phenotype for environment B (A) in the A (B) environment	Ω^B (Ω^A)	0.1	Variable
Probability for a male perfectly adapted to environment A (resp. B) to accepting a female perfectly adapted to environment B (resp. A)	P_C	1	Evolvable
Number of potential partner to choose among	χ	100	Variable
Number of pairwise DMIs	n_{DMI}	50	Variable
Epistasis due to DMIs	ϵ	0.1	Variable
Migration rate	m	0.05	Variable

Table 1: List of parameters and their default values. Status indicates whether the parameter was always constant across all simulations (Fixed), could change between simulations (Variable) or within simulations (Evolvable).

Results

Evolution of strict mate choice or accumulation of genetic incompatibilities depends on migration rate

We identified two possible regimes in the evolution of the three mechanisms of reproductive isolation (RI; Fig. 2). Local adaptation was always the first mechanism to establish, but whether it was followed by the build-up of intrinsic postzygotic genetic barriers (accumulation of genetic incompatibilities) or the evolution of prezygotic barriers (strict conspecific mate choice) depended on the migration rate. Although the mean phenotypic values decreased as migration rate increased, migration did not prevent local adaptation, as a large proportion of individuals had phenotypes close to the optimum and similar to the ones of isolated individuals (Fig S3). We noticed that local adaptation stopped occurring in some replicates when migration became close to extrinsic hybrid load $(1 - w_{ext}^{F1})$ (Fig. S4). We did not find any case where the three barriers evolved simultaneously consistently across all 100 replicates (Fig. 3A). There were only 27 cases out of 890 where local adaptation, strict mate choice, and non-negligible hybrid load evolved between populations (using the minimum mean hybrid load or choosiness observed in isolation as thresholds - i.e., hybrid load > 0.097 and choosiness < 0.034).

In the absence of migration, populations evolved toward their phenotypic optimum. In the limited migration regime, once local adaptation has evolved, it was followed by the accumulation of DMIs, but no evolution of mate choice. This regime of local adaptation, (almost) random mating and DMIs accumulation across populations extended to low migration rates, with the threshold depending on the dispersal stage (up to $m < 5 \times 10^{-5}$ for "adult dispersal" and $m < 5 \times 10^{-4}$ for "juvenile dispersal", Fig. 3, S5). Mate choice behaved neutrally in this context, but was displaced to values lower than $P_C = 1$ by mutational bias. Indeed, with limited migration, evolving towards strict assortative mating $(P_C \to 0)$ was neither advantageous due to the population being relatively homogeneous, nor was being choosy costly, since males were allowed to consider multiple females when reproducing (i.e., for $\chi > 1$ the mutational load, due to standing genetic variation, was larger than the cost of being choosy, Fig. S6). Due to isolation, as expected, DMIs accumulated between populations by chance, although this was limited by several factors. First, purifying selection within each population, prevented mutations to coexist at each pair of interacting loci (i.e., if allele A_1 was fixed, mutation from b_1 to B_1 created a mutational load and was therefore selected against). Second, due to back mutations, fixed incompatible derived alleles (e.g., A_1) could mutate back to compatible ancestral alleles (e.g., a_1) at each DMI pair of loci. Third, since incompatible alleles were also involved in local adaptation, they could be under positive or negative selection, depending on the genetic background and environment.

In the moderate to high migration regime, once populations became locally adapted, strict mate choice evolved, but surprisingly, despite evolution of prezygotic barriers, there was almost no accumulation of DMIs. This corresponded to a regime of local adaptation, strict assortative mating and few or no DMIs. The evolution of strict mate choice ($P_C <$

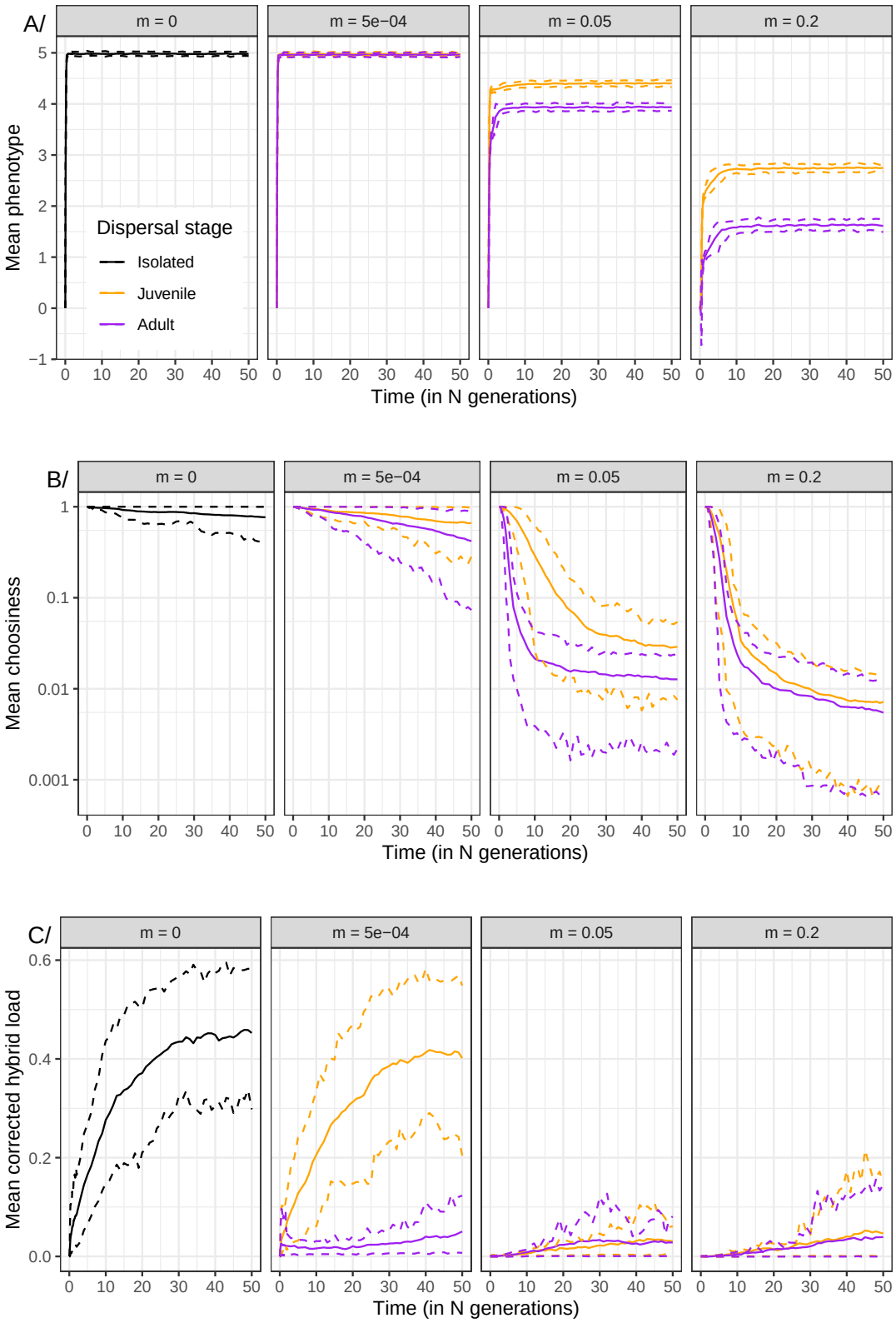

Figure 2: Evolution (in population A) of the phenotype (panel A), mate choice (B; on a log scale) and corrected hybrid load (C) for different migration rates (given in the header) and different dispersal stages. The solid lines correspond to the mean over the 100 replicates, and the dashed lines to the 10th and 90th percentiles. Relation between the evolution of mate choice and corrected hybrid load are displayed in Figures 3 and S8. Stronger RI barrier corresponded to convergence of mean phenotype to 5, mean choosiness to 0 and mean corrected hybrid load to 1. The genetic map used was the "default", populations started in the "ancestral" state and other parameters correspond to the default values given in Table 1.

10^{-2}) can be explained by matings between individuals, adapted to the two environments, producing individuals with both unfit phenotypes (low extrinsic fitness component), and with potential expression of DMIs (low intrinsic fitness component). Thus, there was a strong selective pressure towards the evolution of assortative mating to avoid such unfit matings. Conversely, under these conditions, gene flow was still prevalent enough to prevent the accumulation of DMIs.

That is, we found that despite strong extrinsic and pre-zygotic barriers to gene flow, both in terms of local adaptation (the optimum phenotype of environment A was $\sim$ 10x fitter than an immigrant with the optimum phenotype of environment B, but only 1.78x fitter than the F_1 phenotype), and mate choice (a male at optimum phenotype of A will accept mating with a immigrant female with the optimum phenotype of B in $\sim$ 1% cases), in most cases the between-population hybrid load remained close to 0 when migration rate was higher than 0.005. We expected that incompatible alleles expressed in F_1s would create an intrinsic hybrid load that became stronger with increasing migration rates, due to a higher proportion of F_1 individuals. However, provided that there was sufficient gene flow (i.e., through F_2s and further backcrosses), selection against incompatible alleles involved in DMIs should prevent their accumulation (seen for $m \geq 0.005$). Alternatively, very strict mate choice could result in a low mean hybrid load if immigrants behave as an isolated populations in the alternative environment. This was not the case, as the presence of gene flow was further confirmed by the multimodal distribution of phenotypes after $50N$ generations (Fig. S3), with peaks corresponding to F_1 individuals (phenotypic value close to 0), and backcrosses with intermediate phenotypes (F_2s around ± 2.5). The absence of incompatible alleles at DMI loci was further confirmed by checking the genomes of individuals (after $50N$ generations; Fig. S7). Remarkably, in a few instances, gene flow was likely sufficiently reduced by very strict mate choice ($P_C < 10^{-3}$, Fig. 3), as we saw that DMIs started accumulating (e.g., for $m = 0.2$, 31 in 200 simulations ended with a corrected hybrid load > 0.097, but 23 out of the 26 cases when $P_C < 10^{-3}$).

The dispersal stage influenced the migration rate at which we saw a transition between the two regimes (Fig. 3B), with a lower migration rate threshold with "adult-dispersal". This is expected because immigrating individuals with maladapted phenotypes were more likely to mate in the "adult dispersal" regime (their fitness depends on their birth environment), leading to stronger selective pressure to avoid them. Interestingly, we did not find a parameter space where both strict mate choice and DMI evolved simultaneously (and consistently) at significant strength (Fig. 3B, no values of m with a majority of purple points). This suggested that selection against incompatibilities was more effective than selection for stricter mate choice. Yet, within a given set of parameters, we observed a correlation between stricter mate choice and higher hybrid load, suggesting a trend for the two mechanisms to coevolve, in particular for moderate to large migration rate (Fig. S8). This was likely a consequence of evolution of mate choice: once it became strict enough ($P_C < 10^{-3}$), gene flow was sufficiently reduced such that the two populations behaved as isolated, and DMIs would start accumulating (Fig. 3, S9). As a consequence, we expected reinforcement (i.e., the evolution of strict mating due to genetic incompatibilities) to be unlikely under our model.

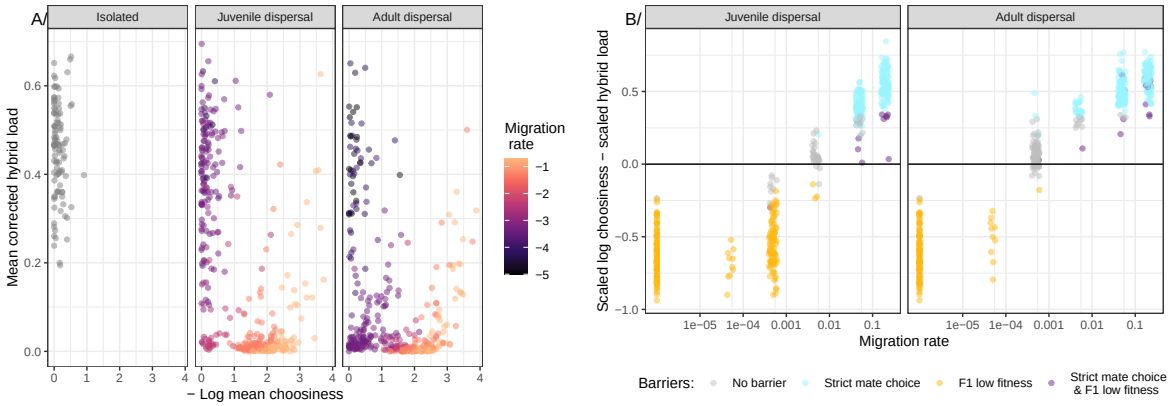

Figure 3: Evolution (in population A) of strict mate choice and accumulation of DMIs are (mostly) exclusive and depends on the migration rate. A/ Relation between (-log) choosiness (strict mate choice corresponds to large values) and mean corrected hybrid load (higher values indicate DMI accumulation) at the end of the $50N$ generations. Color indicates the migration rate (on a log-scale). A detailed figure of this relation per migration rate is given in Figure S8. B/ Relative contrast between scaled log choosiness (defined between 0 (no mate choice) and 1) and scaled hybrid load (defined between 0 (no hybrid load) and 1) as a function of migration rate ($m + 10^{-6}$ on a log-scale) and dispersal stage. Color indicates whether the RI mechanism has evolved (compared to the minimum values observed in isolation). Other parameters correspond to the default values and are given in Table 1.

To further confirm the absence of reinforcement, we investigated secondary contact cases, with or without initial strict assortative mating. We found that post-zygotic barriers due to DMIs erode over time, but with two different regimes (Fig. 4). When secondary contact occurred between populations without initial mate choice ("SC" starting with $P_C = 1$), we found that the evolution of mean choosiness towards strict mate choice was similar to when two populations diverged from an ancestral population ("Ancestral"), and the hybrid load due to DMIs converged to similarly low values (mean hybrid load ≤ 0.10) in both scenarios (Fig. 4 left vs mid panels). In contrast, when secondary contact occurred between populations already with DMIs and strict mate choice ("SC + initial mate choice" starting with $P_C = 10^{-4}$), we found a distinct dynamics, with maintenance of very strict mate choice for scenarios with high migration ($m > 0.05$), and evolution of hybrid load towards high equilibrium values (mean hybrid load ~ 0.35), irrespective of the migration rate.

The post-zygotic barrier due to DMIs eroded over time under all considered scenarios, either towards the hybrid load equilibrium (see next section) if strict assortative was initially present ("SC + initial mate choice"), or until it was mostly gone ("Ancestral" and "SC"). We note that erosion of the post-zygotic barrier due to DMIs happened relatively slowly over time, indicating that DMIs were removed rather than not expressed due to population substructure within each environment. Overall, this indicates that reinforcement (as defined above) is not possible under the investigated scenarios, due to the effective removal of DMIs when there is enough gene flow ($m \geq 0.005$), consistent with previous theoretical work on continent-island models (Agrawal et al., 2011; Bank

et al., 2012).

Interestingly, we found that mate choice and DMIs could not maintain population differentiation in absence of local adaptation in secondary contact models (Fig. S11). At high migration rate, the lack of differentiation was not caused by a collapse of RI, but through initial ecological exclusion of one of the two populations (Fig. S11, S12). Once one of the populations was lost, the role of mate choice and genetic incompatibilities became irrelevant and individuals in the two environments behaved as a single population. In contrast, at low migration rates ($m \leq 5 \times 10^{-4}$), we found that phenotypic differentiation converged to zero at similar rates for cases with and without migration, indicating that this is due to mutational bias (see Appendix). However, ignoring cases where ecological exclusion occurred, DMIs were actively purged with migration, as the hybrid load converged to zero (Fig. S11).

For comparison with our results assuming a shared genetic basis for the three RI mechanisms, we considered additional models where at least one of the barriers was decoupled. First, we considered the "neutral display" map with $n_t = 2$ phenotypic traits, where the first trait determined local adaptation (but not affecting mate choice) and the second trait used for assortative mating (but not under ecological selection). Under these conditions, although local adaptation evolved, mate choice was unable to evolve from an ancestral state nor from a secondary scenario (Fig. S13). Even when starting from secondary contact with initial mate choice (initial $P_C = 10^{-4}$), choosiness was slowly eroded, and populations converged to the same phenotypic value at the assortative mating trait. The loss of the DMIs always occurred first and seemed to be the trigger that led to the loss of mate choice. This was further confirmed by considering instances of increasingly costly DMIs (larger ϵ): strict choosiness remained longer or persisted, as F_1s had a lower intrinsic fitness and hence were unlikely to be picked as potential mating partners (Fig. S14). Second, we considered the "neutral" map with distinct loci for DMIs and for the phenotype under ecological selection (also involved in mate choice). Under these conditions, the evolution of local adaptation, mate choice and the proportion of DMIs between populations was similar to the "default" case, in which DMI involved loci affecting the phenotype (Figure 5).

No accumulation of DMIs with migration and lack of snowball effect, irrespective of the network of DMI interactions

Across migration rates, the intrinsic hybrid load was either absent or evolved towards some non-zero equilibrium value (Figure 2C). In the later case, the hybrid load matched what was observed in the absence of gene flow ($m = 0$), and could be obtained starting from an ancestral population or a secondary contact scenario. Such equilibrium hybrid load was equivalent to having five DMI pairs differently fixed between the two populations. This indicated that in scenarios where DMIs did accumulate, only about 10-15% of all possible DMIs were differently fixed between the two populations (in terms of equivalent number of DMIs), without a clear snowball effect (Orr, 1995), which predicts a faster than linear increase in the number of DMIs through time (Fig. S15). This could be partially

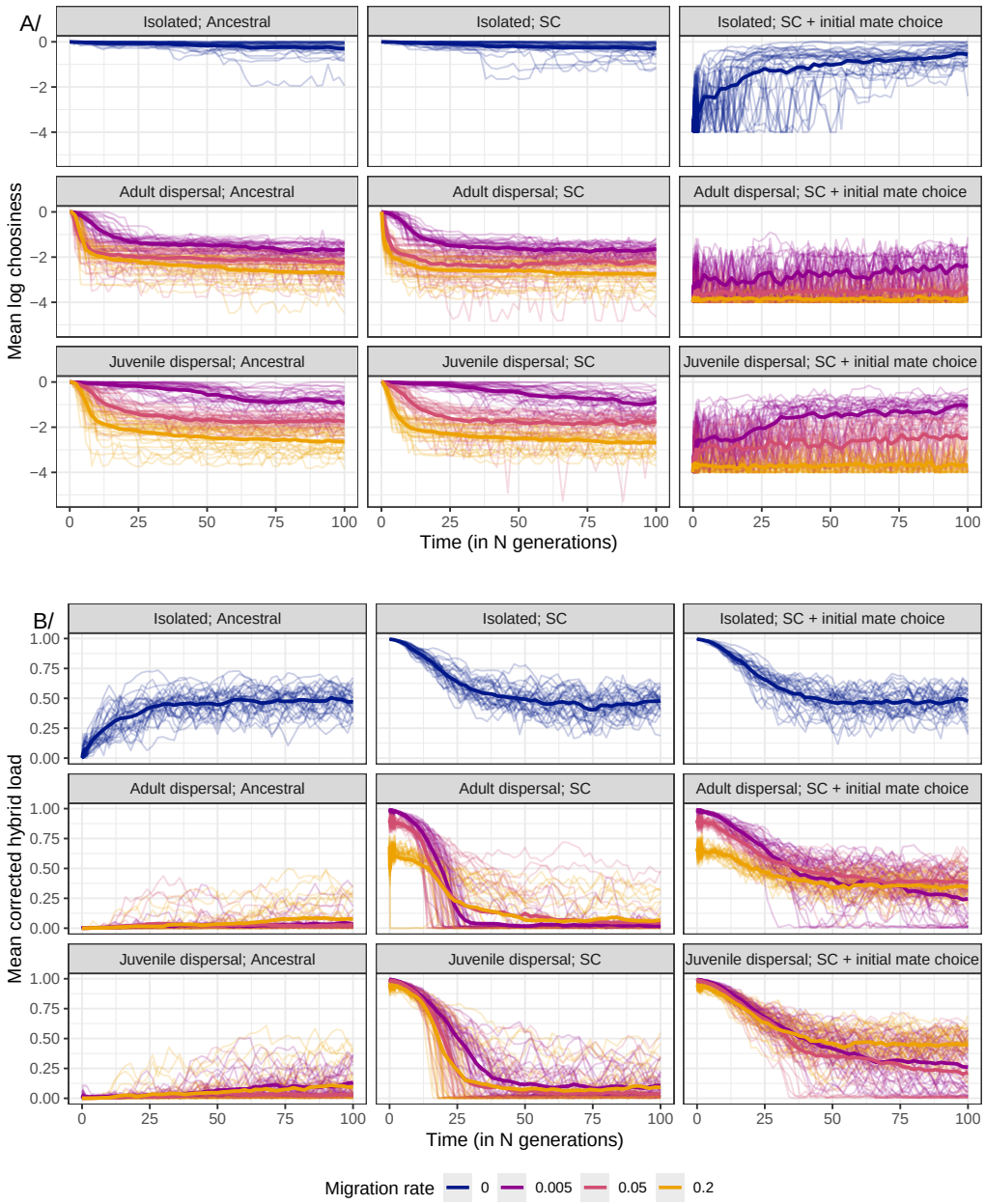

Figure 4: Evolution (in population A) of mate choice (panel A) and corrected hybrid load (B) for different dispersal stages and different starting conditions: the "Ancestral" (default) scenario, the secondary contact ("SC") scenario and the secondary contact with initial mate choice scenario ("SC + initial mate choice"). Different migration rate are given indicated by different colors, with each thin line corresponding to a different replicate and the thick line to the mean over the 30 replicates. The final states and link between mate choice and hybrid load are displayed in Figure S10. Other parameters correspond to the default values and are given in Table 1

explained by the design of the genetic architecture and mutation process, as forward and backward mutation rates (at each biallelic locus) were considered equal.

To understand why only 10 to 15% of the DMIs were differentially fixed, we considered a simple deterministic model describing how DMIs would accumulate between populations in the limit of weak mutation and strong selection (i.e., strong epistasis, $\epsilon \to \infty$). In each population, at equilibrium and assuming a low mutation rate, about half of the loci would be fixed for the derived allele (i.e., A_i or B_i at loci A and B of DMI pair i) and the other half for the ancestral allele (i.e., a_i or b_i). In addition, for each DMI pair, the derived alleles (A_i or B_i) could only arise in the ancestral background, whereas the ancestral alleles could arise in any background. Under these conditions, the population had three possible states: fixed for a_ib_i, A_ib_i or a_iB_i. The expected probability of having A_i fixed in the first population at a given time-point was $P(A_i \text{ in } p_1) = \frac{1}{3}$ (see Appendix for details). Therefore, the probability of having a DMI between the two isolated populations was $\frac{2}{9}$, while in the absence of back mutation, this probability rise from $\frac{2}{9}$ to $\frac{1}{2}$.

We observed a lower number of DMIs in the simulations than predicted by the weak mutation strong selection approximation. This was the case irrespective of the epistasis strength ($\epsilon = 0.9$ or $\epsilon = 0.01$, Fig. S16), or the genetic map ("default", "neutral","network" or "optimized" maps). Yet, we found that the scaled mutation rate (i.e., $\theta = 4N\mu$) influenced the proportion of equivalently fixed DMIs (Fig. S17). These results suggested that, in large populations or when mutation rate is high, multiple mutations might segregate at the same time within each population. If both A_i and B_i were polymorphic simultaneously in a given population, selection against those incompatible alleles would prevent their fixation. Indeed, in isolated populations at generation $50N$, almost 40% of all pairs of DMIs had both alleles A_i and B_i segregating in the population, yet with the rarer among the two alleles never exceeding a frequency of 0.015 (Table S1).

We further investigated whether the DMI architecture could explain the lack of a snowball effect. The snowball effect predicted by Orr (1995), is expected to be mediated by whether incompatible loci are involved in a single or multiple DMIs (Guerrero et al., 2017). We thus compared the "neutral" architecture (loci forming DMIs were not affecting the phenotype), the "network" architecture (each locus could be involved in more than one pair of DMIs and were not affecting the phenotype), and the "optimized" architecture (for each DMI pair the A_i allele at locus A_i had a negative phenotypic effect in environment B, and the allele B_i at locus B_i had a positive phenotypic effect in environment B). We found evolution towards lower hybrid load values for the "network" than the "neutral", "default" and "optimized" architectures, suggesting that the lower the number of underlying DMI loci, the lower the number of equivalent fixed DMIs (Fig. 5B). In the "network" architecture, each locus was involved on average in 8 DMIs pair, increasing the selective pressure caused by mutation (by a factor ≈ 8) and preventing the fixation of derived alleles, even in the absence of gene flow. Indeed, under the "network" architecture, we did not find an accumulation of DMIs, even in scenarios without migration. In contrast, for the "optimized" architecture, despite the fact that DMIs were fully correlated with the phenotypic effect of alleles, the proportion of equivalent fixed DMI evolved towards values similar to the "default" architecture (≈ 0.15). Importantly, with migration, accumulation

of DMIs was strongly limited in all investigated DMI architectures.

Gene flow mostly caused by immigrant individuals of the choosy sex

Due to the implementation of the mate choice scheme, we expected that a male ("choice-making" individual) would have a higher chance to leave offspring after moving to the alternative environment than a female ("non-choosing") individual, all things being equal. This arose because a male, once selected as a potential mate based on its intrinsic and extrinsic fitness, only needed to accept one among χ potential mates, while a female, once chosen as a potential mate, had only one chance to be accepted for mating. Assuming all individuals were at the optima in each environment, this difference could easily be quantified, considering that the resident population have a size $2N$ with 50:50 sex-ratio, all resident individuals have fitness w_r, and that the focal immigrant individual has fitness w_f. Under these assumptions, the probability that this focal individual left offspring in the next generation is, for a focal male:

$$P_m(desc.) = 1 - \left(\frac{(N-1)w_r}{w_f(1-(1-P_C)^\chi) + (N-1)w_r}\right)^{2N} \xrightarrow[N\to\infty]{} 1 - e^{2((1-P_C)^\chi - 1)\frac{w_f}{w_r}} \quad (5)$$

and for a focal female:

$$P_f(desc.) = 1 - \left(\frac{(N-1)w_r}{P_C w_f + (N-1)w_r}\right)^{2N} \xrightarrow[N\to\infty]{} 1 - e^{-2P_C\frac{w_f}{w_r}} \quad (6)$$

where P_C is the probability of a male accepting a mating with a female with an alternative phenotype, and χ is the number of potential mates considered by a male to reproduce with (details of the calculations are given in the Appendix). These predictions matched simulations (Fig. S18), including under complete neutrality ($w_r = w_f = 1$, $P_C = 1$) and random mating. Given these equations, immigrating focal females were far less likely to leave immediate descendants than their male counterpart, as the probability for females did not depend on the number of mating attempts χ (Figure 6). In contrast, the probability of leaving descendants for males increases as the number of attempts to mate χ increases. Thus, focal males and females are expected to have similar probabilities of leaving descents only when the cost of choosiness is extremely high ($\chi = 1$). In contrast, under strong choosiness ($P_C \to 0$) and weak choosiness cost ($\chi \to \infty$), gene flow is expected to be sex-specific, mostly driven by the choosy sex. Since we fixed $\chi = 100$, in all our simulations gene flow was mediated mostly by males.

Local adaptation as the main barrier to gene flow in scenarios with migration

To quantify the barriers to gene flow we computed the mean sojourn times of a neutral allele from a focal immigrant individual. Regardless of the migration rate at which populations evolved, the mean sojourn time of an unlinked neutral marker was usually lower or similar to the expected sojourn times under neutrality, indicating that some RI

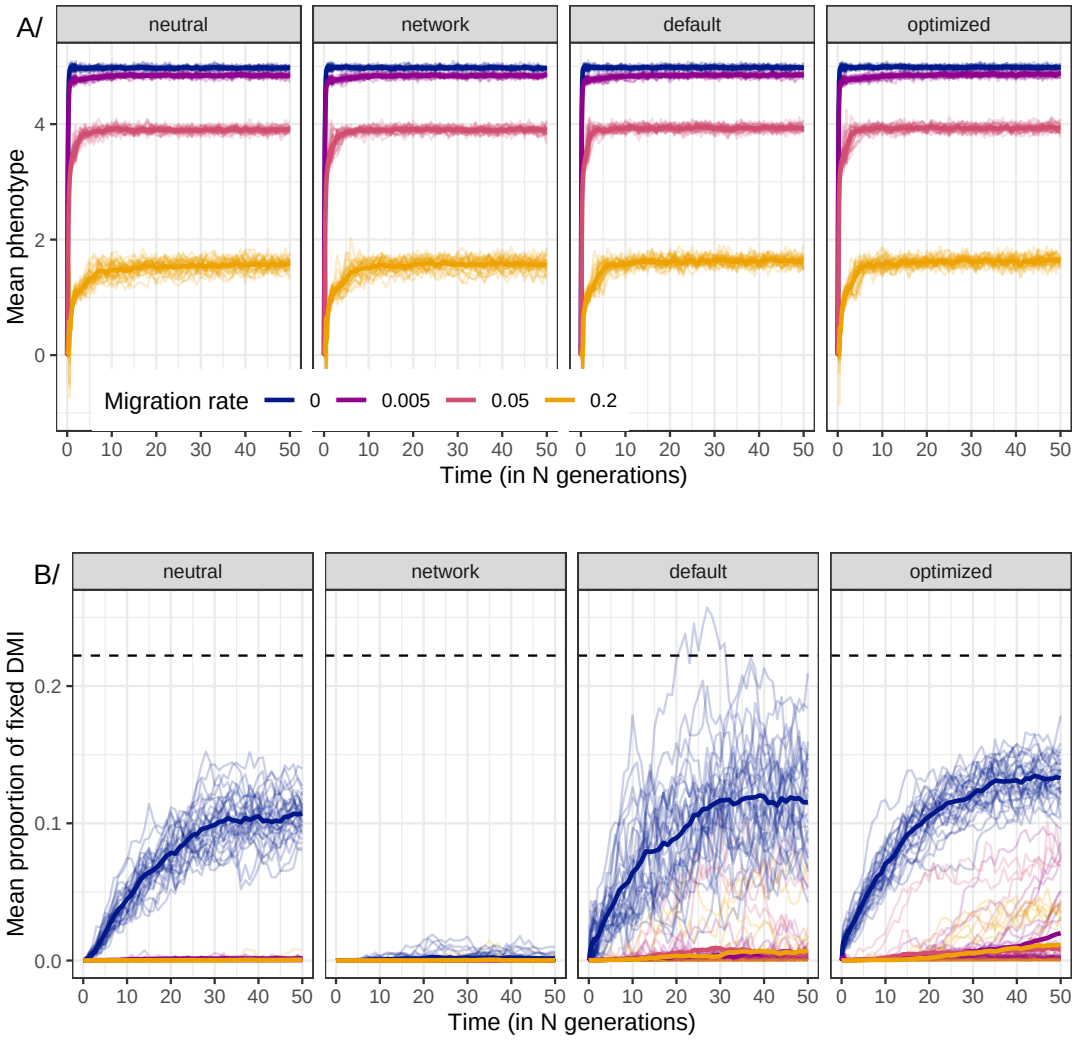

Figure 5: Evolution (in population A) of the phenotype (panel A) and number of equivalent fixed DMIs (B; computed according to equation (4)) for different DMIs architecture (given in the header) and different migration rates. Each thin line corresponds to a different replicate, with the thick line corresponding to the mean over the 30 replicates. Color corresponds to different migration rates: $m = 0$ in blue, $m = 0.005$ in purple, $m = 0.05$ in pink and $m = 0.2$ in orange. For the B panel, the black dashed line corresponds to the weak mutation strong selection approximation for the proportion of DMI fixed between populations, $\frac{2}{9}$. The "default" network corresponds to the 100 loci out of 500 forming 50 pairs of DMIs, the "network" one to 50 loci out of 800 forming 200 pairs of DMIs, and the "optimized" one to 500 loci out of 500 forming 250 pairs of DMIs, with always an allele increasing the phenotypic value interacting with one decreasing it (see methods). Other parameters correspond to the default values and are given in Table 1

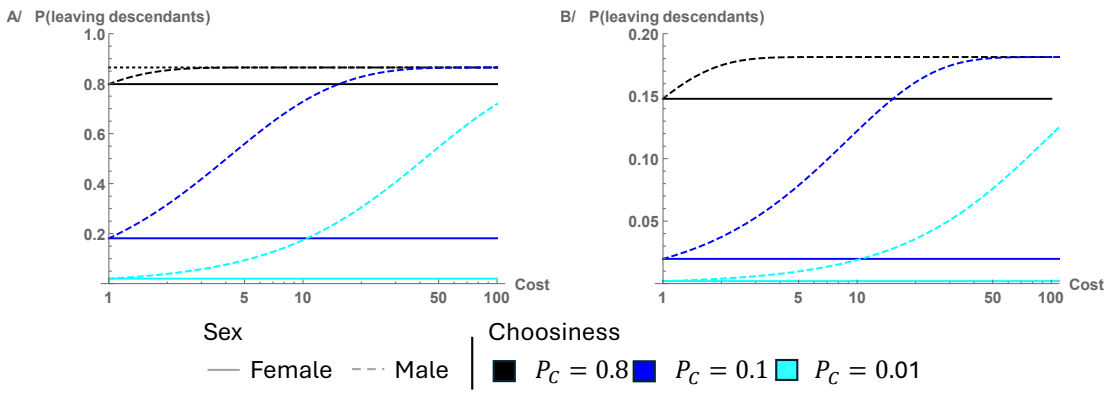

Figure 6: Probability of a focal immigrant individual (fitness w_f) to leave at least one descendant in a resident monomorphic population (fitness w_r) in the next generation ($P(desc.)$ as a function of the cost of choosiness χ, in the absence (panel A, $w_f = w_r$) and presence (B, $w_f = 0.1$, $w_r = 1.0$) of local adaptation. We represent this probability for a focal male (dashed line; eq. 5) and female (eq. 6 solid line) and difference choosiness strength ($P_C = 0.8$ in black, $P_C = 0.1$ in blue and $P_C = 0.01$ in cyan). The probability for the neutral case is given by the dotted dashed line on panel A and is not displayed on panel B due to scale. Other parameters are $N = 1000$ and $w_r = 1$.

barriers effectively reduced gene flow (e.g., local adaptation) where other did not or did not evolve (e.g., mate choice at low migration rates, and genetic incompatibilities at high migration rates, Fig. 7). The combination of barriers was not directly antagonistic since the combination of barriers always decreased the mean sojourn time compared to the effect of each barrier individually. This result was qualitatively the same if we considered a linked neutral marker instead (Fig. S19). This was the case regardless of the sex of the focal individual, although the choosy sex (males) had longer sojourn times when mate choice was involved ("MC", "LC+MC", "MC+DMI", "all"), consistent with higher gene flow when immigrants were of the choosy sex (see previous section).

Across all combinations of barriers and dispersal stages, the shortest sojourn times were similar irrespective of the migration rate, indicating that RI barriers evolved to similar levels with and without migration. Irrespective of the dispersal stage and migration rates, cases where all barriers were active ("all") showed shorter sojourn times, i.e., stronger barriers. Yet, cases with local adaptation ("LA"), local adaptation and mate choice ("LA+MC") and local adaptation and genetic incompatibilities ("LA+DMI") often led to similar sojourn times to those found by combining all barriers ("all"), although this depended on the migration rates and dispersal stage. In agreement with purging of DMIs, when migration $m \geq 0.05$, the sojourn times when only the DMI barrier was active ("DMI") were similar to neutral. In contrast, without migration, DMIs evolved successfully and acted as a RI barrier reducing sojourn times to ≈ 0.40 of the values observed under neutrality.

Interestingly, across most scenarios we found differences depending on the dispersal stage in the reduction of gene flow (Fig. 7). First, for scenarios with local adaptation ("LA", "LA+MC", "LA+DMI", "all"), the reduction in sojourn time was stronger for "juvenile dispersal" than "adult dispersal", i.e., local adaptation was a much stronger

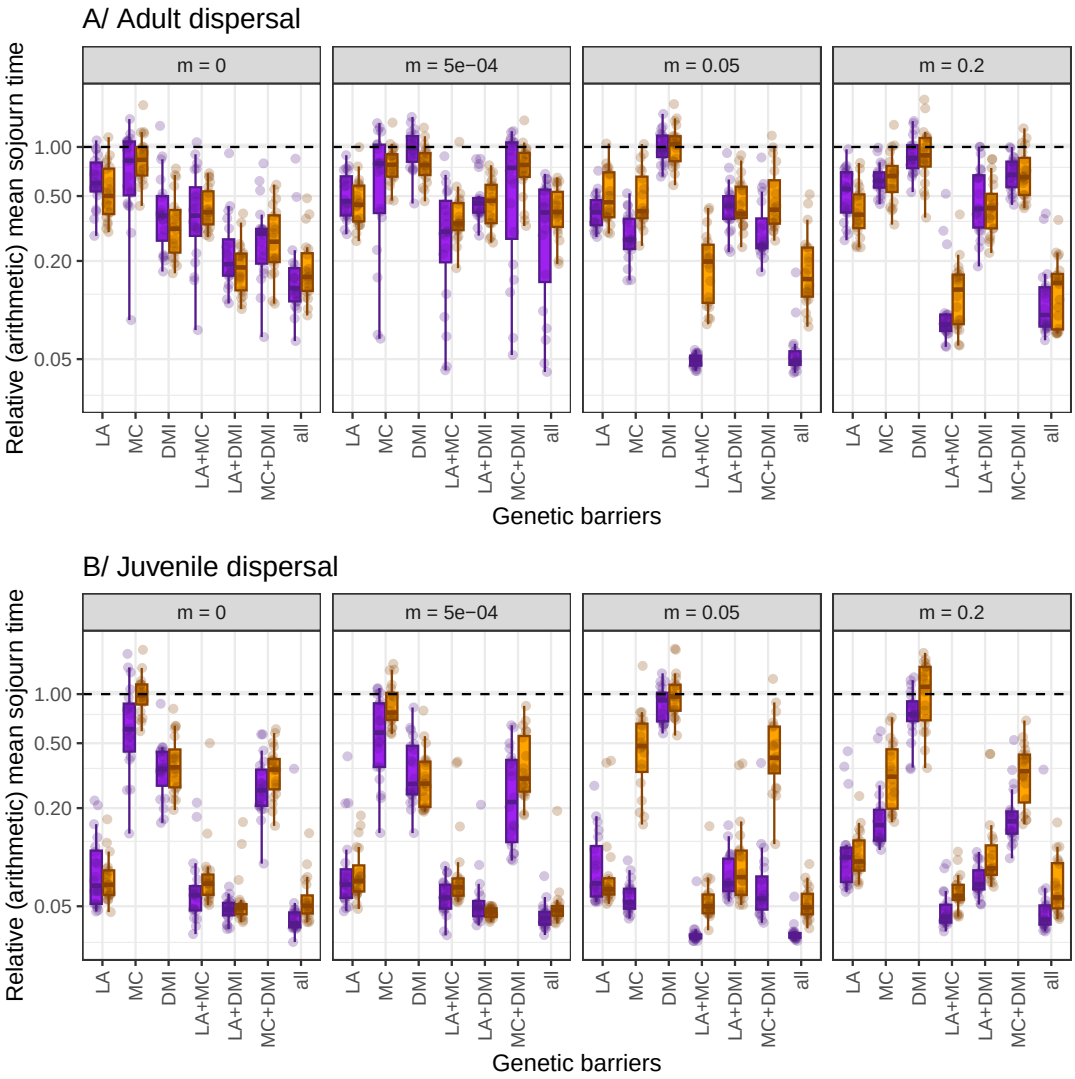

Figure 7: Impact of reproductive isolation (RI) barriers on the relative sojourn time of neutral alleles at a freely recombining marker introduced by a focal immigrant individual. We considered the mean sojourn time as a proxy of the barrier strength, with lower values indicating stronger barriers against gene flow. Relative sojourn times were obtained by turning off barriers, and the x-axis indicates which barriers were kept active: local adaptation (LA), mate choice (MC), post zygotic isolation (DMI), a combination of two (e.g., LA+MC) or all three barriers together (all). Results shown for a male (orange) and female (purple) focal immigrant individual. Sojourn times were measured relative to the mean sojourn time under neutrality across all replicates, i.e., neutrality corresponds to a value of 1 (dashed horizontal line). Lower values indicate less introgression. Panel A corresponds to the "adult dispersal" stage and panel B to the "juvenile dispersal" one. Additional migration rates are displayed in Fig. S20. The corresponding figures for the absolute times (Fig. S21), and for the relative sojourn time of a linked marker (Fig. S19) are given in Supplement. Other parameters correspond to the default values.

barrier to gene flow with "juvenile dispersal". Second, for "juvenile-dispersal", when all mechanisms were active ("all"), the reduction in sojourn time was mostly independent of the migration rate and of the sex of the focal immigrant individual, since focal individuals failed to reproduce in the first generation. For "adult-dispersal", this was no longer the case, as sojourn times depended on migration rate and sex of focal individual (strongest joint effect for "all" barriers observed for $m = 0.005$, Fig. S5). The evolution of stronger barriers at intermediate migration rates with "adult-dispersal" was due to a balance between two mechanisms: increasing migration triggered the evolution of mate choice, but also ensured that at each generation there was a proportion of individuals with the alternative phenotype in the resident population. As migration further increased, this proportion individuals with the alternative phenotype became sufficiently large, that the focal immigrant was likely to successfully reproduce. Therefore, under the "adult dispersal" life cycle, we predict that strong barriers to gene flow leading to speciation would only evolve for scenarios with the "right" amount of migration.

A high variance (overdispersion) for the mean sojourn time under some scenarios was observed, mainly for barriers involving mate choice ("MC", "LA+MC", "MC+DMI", "all") and for intermediate migration rates ($m = 0.0005$ and $m = 0.05$). This overdispersion reflected stochasticity across replicates, since in some replicates, populations evolved strong mate choice, while not in others.

Finally, we investigated the sojourn time of neutral alleles in scenarios of secondary contact with preexisting choosiness and fixed levels of the strength of each barrier, thus removing the stochastic variation in evolution of barriers across runs. With "juvenile dispersal", local adaption remained the strongest barrier to gene flow, i.e., shorter sojourn times for "LA" (Fig. S22), with addition of mate choice ("LA+MC") further reducing the sojourn times (but only in females, and when each barrier was relatively weak). Genetic incompatibilities ("DMI") were the weakest of all barriers, providing shorter reductions in sojourn time than the other mechanisms, but equivalent to mate choice ("MC") in the choosy sex. With "adult dispersal", local adaptation ("LA") was one of the weakest barriers. Surprisingly, although with "juvenile dispersal" genetic incompatibilities ("DMI") were one of the weakest barriers, with "adult dispersal" "DMI" provided the strongest barrier (i.e., shorter sojourn times), even stronger than local adaptation and without sex-specific effects.

Discussion

We investigated how the interaction of different mechanisms of reproductive isolation (RI) impacts divergence and gene flow between populations, under a polygenic model of local adaptation and genetic incompatibilities with a shared genetic architecture. For the evolution of RI, Table 2 provides a summary of general trends observed. In scenarios with migration, local adaptation was unsurprisingly always the first barrier to evolve, with either accumulation of genetic incompatibilities (DMIs) or the evolution of strict assortative mating evolving afterwards. The evolution of the last two barriers were somewhat mutually exclusive: whether strict mate choice or accumulation of DMIs evolved

Genetic architecture	Initial conditions	Phenotypic divergence	Evolution of strict mate choice	Accumulation of DMIs
Default	Ancestral	Yes (approx. up to $m=1-w(F_1)$) Fig 2; Fig S4; Fig S5	If migration is strong enough Fig 2; Fig S5	If migration is weak or very strict mate choice has evolved Fig 2; Fig 3; Fig S5
	Secondary contact	Yes	If migration is strong enough Fig 4A	If migration is weak or very strict mate choice has evolved Fig4A
	Secondary contact with initial mate choice	Yes	Remained (if no isolation) Fig 4B	Maintained at a mutation selection equilibrium if mate choice remains sufficiently strict Fig 4B
Default - no LA	Secondary contact with initial mate choice	No; Ecological exclusion for $m \geq 0.005$ or for $m \leq 0.0005$ converge to ancestral state due to mutational bias Fig S11; Fig S12	No; Evolving toward choosiness values above 0.1 Fig S11; Fig S12	No; Lost either due to ecological exclusion for $m \geq 0.005$ or purged by selection if $0 < m \leq 0.0005$ Fig S11; Fig S12
Neutral display	Ancestral	Yes at the selected trait; No at the cue trait Fig S13	No Fig S13	Only if m is really low Fig S13
	Secondary contact	Yes Fig S13	No Fig S13	Only if m is really low Fig S13
	Secondary contact with initial mate choice	Yes Fig S13; Fig S14	Maintained if epistasis caused by DMI is strong enough - loss of MC triggered by the loss of DMI Fig S13; Fig S14	Maintained at a mutation selection equilibrium if epistasis caused by DMI is strong enough Fig S13; Fig S14
Neutral	Ancestral	Similar to default case Fig 5	Similar to default case	Similar to default case Fig 5
Network	Ancestral	Similar to default case Fig 5	Similar to default case	No Fig 5
Optimized	Ancestral	Similar to default case Fig 5	Similar to default case	Similar to default case Fig 5
Default 3D	Ancestral	Same as default case if corrected for the distance between optimum Fig S23	Similar to default case Fig S23	Similar to default case Fig S23
Default - effect of Q	Ancestral	Overall similar to default case, but with weaker divergence as Q increases Fig S24	Same as default case Fig S24	Overall similar to default case, but with lower hybrid load as Q increases Fig S24
Default 3D - asymmetry of optimums	Ancestral	Similar to default 3D case Fig S25	Similar to default 3D case Fig S25	Similar to default 3D case Fig S25

Table 2: Summary table of our results, indicating the general trend, within the parameter ranges explored. Each row corresponds to different combination of genetic architecture, different initial conditions, and (possibly other parameter changes). We summarized the general trend in the evolution of phenotypic divergence (in most cases a proxy for local adaptation), evolution of strict mate choice, and accumulation of DMIs. Figures supporting the results are indicated below each statement, and not indicated when results were not shown.

was dictated by migration rate, and to a lesser extent by the life cycle. Surprisingly, even in cases where local adaptation and strict mate choice evolved, DMIs acted as a very weak barrier, consistent with purging of genetic incompatibilities provided there was sufficient gene flow. Thus, reduction in gene flow (strength of RI) was mostly a consequence of the action of local adaptation, with mate choice being also effective for cases with sufficient migration. Importantly, we modeled here mate choice as male choice but the model is fully symmetric and all genetic elements were autosomal. Therefore, all conclusions apply to both male and female mate choice.

Local adaption at the center of speciation with gene flow

Under our model with polygenic architectures, local adaptation played a major role in the evolution of RI as it was always the first barrier to evolve. The key role of local adaptation, in models of speciation with gene flow, had already been pointed out previously using two-locus models (Agrawal et al., 2011; Bank et al., 2012). In addition to being the first RI barrier to evolve, with "juvenile dispersal", local adaptation was the main mechanism responsible for the reduction of sojourn times of neutral introgressed alleles, a proxy for the level of gene flow between populations. The importance of ecological speciation has received a lot of attention (as detailed in Nosil, 2012 - but see Anderson and Weir, 2022). Our results are in agreement with the role of local adaptation in ecological and speciation scenarios with gene flow, but bring an important nuance. Indeed, when considering the "adult dispersal" life cycle, local adaptation drives the evolution of phenotypic differentiation between the two populations, and mate choice or accumulation of DMI only evolve once populations become locally adapted. However, provided that populations evolved strict mate choice or accumulated DMIs, the strength of these two barriers becomes similar to local adaptation, as we found for secondary contact models from fixed population states (Fig. S22). For both the evolution from an ancestral population or from secondary contact from fixed population states, the relative strength of local adaptation depended on the life cycle, being stronger with "juvenile dispersal". Since the only difference between the two life cycles was whether the fitness of an immigrant individual was affected or not by the new environment, this indicates that local adaptation is mostly effective upon arrival of the immigrant individual, but becomes ineffective to reduce gene flow when the focal individual successful reproduces. This result highlights the brittle nature of local adaptation/ecological differentiation as a genetic barrier to gene flow (Blanckaert et al., 2020).

Evolution of mate choice when there is sufficient migration

In our model, mate choice was never able to function as an independent barrier. It evolved only in the presence of local adaptation and non negligible migration. Therefore it always evolved as consequence of another barrier, and corresponds to a form of coupling of multiple RI barriers (sensu Butlin and Smadja, 2018).This delay in evolution of mate choice versus local adaptation has been previously reported across different

mate choice models (Thibert-Plante and Gavrilets, 2013) when investigating pre-zygotic barriers exclusively.

Mate choice was also effective at limiting gene flow between species, but only for the non-choosy sex and when a very strict choosiness evolved. This is in line with previous simulations studies, highlighting the relatively ineffective role of assortative mating to maintain a narrow hybrid zone between populations (Irwin, 2020). As in Irwin (2020), our results partly stem from modeling choosiness using a Gaussian function and a matching phenotype approach. In particular, this implies that mating of F_1s with identical phenotypes is very likely, and F_1s are also likely to be accepted as potential partners by resident individuals. Our approach to model mate choice creates a "now or never" dichotomy for reducing gene flow, which is seen in differences between the choosy and non-choosy sex. If the focal immigrating individual manages to reproduce, then most of the RI barrier is gone and the introgressed marker behave somewhat similarly to a neutral mutation. Having the choosiness function more akin to a step function instead of a Gaussian could mitigate the effects described here and generate stronger barriers to gene flow. The suitability of each approach depends on whether the trait used for mate choice is qualitative or quantitative. In the later case, a continuous smooth function is a more likely representation of the biological process involved in mate choice (especially since we are not considering the environmental variance that could contribute to the phenotype and would flatten the choosiness function). Importantly, we never observed the evolution of mate choice due to the presence of genetic incompatibilities, as the two mechanisms seem to exist in different parameter spaces. This is likely because the selection against DMIs, caused by the hybrid load, is more sensitive to migration than selection for stricter mate choice, resulting in a disjoint parameter space: combination of parameters where DMI could accumulate did not overlap with the ones where stricter mate choice could evolve. While surprising given that occurrence of the two RI barriers is common in nature, we observed rare cases where both strict mate choice evolved and DMI accumulated. In those rare cases, DMIs accumulated because of the evolution of mate choice, rather than the opposite. In addition, mate choice was not able to evolve if the trait used for assortative matings was not under local adaptation (i.e., if it was not a magic trait), but could persist if F_1s individuals were sufficiently unfit. Finally, we chose to model mate choice as assortative mating, with both males and females being able to engage in multiple matings. This makes the results obtained here valid for both males and females. However, under a different mate choice system such as a preference for a given trait, this symmetry does not exist, with female choice being far more prevalent (Fitzpatrick and Servedio, 2018).

Genetic incompatibilities do not accumulate in locally adapted populations with strict mate choice when there is sufficient gene flow

Two types of incompatibilities were modeled in our approach: extrinsic and intrinsic ones. Indeed, Fisher's Geometric Model naturally generates epistasis between mutations due to the quadratic relationship between phenotype and fitness. Within this framework,

Fraïsse et al. (2016) showed that many empirical patterns of speciation (e.g., Haldane rule, heterosis, hybrid breakdown) can be mimicked, making it a useful model to study RI. However, such approach makes it extremely challenging to characterize the effect of genetic incompatibilities, as they depend both on the environment and the genetic background. Therefore, our model also included intrinsic incompatibilities using the classical Bateson-Dobzhansky-Muller model (Bateson, 1909; Dobzhansky, 1936; Muller, 1942). Assuming that the same locus affecting local adaptation can generate genetic incompatibilities may seem to be a strong hypothesis, yet examples of local adaptation generating DMIs have been reported (Macnair and Christie, 1983; Świadek et al., 2017; Frayer et al., 2025). In particular, adaptation of *Saccharomyces cerevisae* to low glucose medium (Anderson et al., 2010; Kvitek and Sherlock, 2011) or nyastin (Ono et al., 2017) reveals the existence of genetic incompatibilities between beneficial mutations. The same pattern was also observed in *Methylobacterium extorquens* (Chou et al., 2014). Regardless, we obtained the same results when the DMIs affected neutral loci, or when the architecture was "optimized" to favor DMI accumulation, suggesting that DMIs acted more as a constraint to local adaptation instead of the later favoring their accumulation.

Generally, under our model, genetic incompatibilities seems to arise more as a consequence of isolation (either due to low migration rates or strong reproductive barriers), and not as an active mechanism to prevent gene flow, matching the predictions from the two-locus model (Bank et al., 2012). Our results also matched with the outcome of experimental evolution in *Saccharomyces cerevisiae*, where Dettman et al. (2007) observed the evolution of DMIs as a by-product of divergent selection between isolated populations. The same pattern was also observed in experimental evolution of isolated populations of *Neuspora* (Dettman et al., 2008). Whether such accumulation of DMI as a by-product could happen with ongoing gene flow remain largely unexplored (Kulmuni and Westram, 2017). Our study reveals a duality in the effect of these intrinsic genetic incompatibilities in the speciation process. Accumulation of DMIs is relatively constrained, only happening when gene flow was absent or limited. This effect was further amplified when forward and backward mutation rates were symmetric, as the within-population mutational load generated by the possible DMIs tend to select against the fixation of any of the incompatible alleles (Fig S17), even in the absence of migration.

Despite this, multiple DMIs have been reported across many organisms (Presgraves, 2003; Kao et al., 2010; Corbett-Detig et al., 2013; Powell et al., 2020; Frayer et al., 2025), including a characterization of the underlying genetic mechanisms (reviewed in Table 1 of Kitano and Okude, 2024). Potentially, all of these DMIs may have formed in isolation, as described in the conceptual definition of the DMI model (Coyne and Orr, 2004) whether due to temporal, geographical or prezygotic barriers. However, isolation is rather unlikely, as gene flow has been reported for some of the cases mentioned above (e.g., between *Xiphophorus malinche* and *X. birchmanni* Powell et al., 2020). Alternatively, it is possible that DMIs accumulation happens at a much slower rate, as discussed for cichlids (Stelkens et al., 2010), that was not captured with our design here. Finally, DMIs are often thought as fixed differences between species. Yet as argued by Cutter (2012) and demonstrated in *Drosophila melanogaster* Corbett-Detig et al. (2013), this may not be

the case, and many genetic incompatibilities may be segregating within populations - a feature that we recovered in our simulations (Table S1).

Under our model, as soon as migration was non negligible, genetic incompatibilities were unlikely to accumulate between populations, despite the evolution of phenotypic differentiation and strict mate choice. Interestingly, this pattern has been observed in nature in cases of ecological divergence. For example, cichlid fish species maintain their integrity despite coexisting with gene flow in at least parapatry, and in the presence of mate choice, yet hybrid breakdown remained limited (Stelkens et al., 2015) and DMIs accumulation happened at a much slower rate than speciation (Stelkens et al., 2010). Such pattern also matches the example of *Anopheles gambiae* and *A. coluzzi*. As summarized in Mallet and Mullen (2022), the two species display ecological differences and strong assortative mating, but are sympatric and apart from a few islands of differentiation, 99% of the genome is homogenized, and therefore not propitious to the accumulation of DMIs (Turner et al., 2005; Lee et al., 2013). The lack of characterized DMIs may be partly due to the challenge associated with their detection (Nouhaud et al., 2020; Blanckaert and Payseur, 2021), but our model here also highlights that low levels of gene flow between populations are sufficient to purge DMIs.

Finally, it is possible that some of the assumption of our model may limit the accumulation of DMIs. First, we are assuming a constant population size and therefore soft selection (Wallace, 1968, 1975) - low fitness phenotypes therefore have a higher chance of leaving offspring when frequent enough compared to a hard selection scenario. While extinction of either or both population is a non negligible risk, demographics and evolutionary mechanisms have been shown to act in opposite direction with regards to the hybrid speciation process (Blanckaert et al., 2023). Therefore, DMIs may play a more important role when considering hard selection with both demographic and evolutionary mechanisms - such as allowing the populations to be affected by changes in effective population size. Second, mutations were limited to point mutations and structural variants (e.g., inversion, translocation) were not included. These large-effect mutations can be central to local adaptation and ecotype formation (e.g., 22 and 12 putative inversion have respectively been reported in *Littorina saxatalis* and *L. fabalis* (Johannesson et al., 2024), at least 4 putative inversions in *Coelopa frigida* (Mérot et al., 2021), and 3 inversions in *Heliconius numata* (Jay et al., 2021)), especially in the early stages of speciation (Kirkpatrick and Barton, 2006). Third, we focused on pairwise epistasis. However, higher order epistasis (Ayala-López and Bank, 2025) may play an important role, as it can partially alleviated the within-population mutational load, making the accumulation of DMIs more likely.

Conclusions

We explicitly modeled the interaction between local adaptation, genetic incompatibilities (DMIs) and mate choice, by considering that the same loci could be involved in the phenotype (under selection in the two environments) and associated with DMIs, and that mate choice depended on phenotype and that choosiness was due to a modifier locus

linked to sites determining the phenotype. Surprising, despite a common genetic basis that we expected to favor the joint evolution of all three RI barriers, we found that long term evolution from an ancestral population did not lead to this joint build up, i.e., locally adapted populations with strict mate choice and accumulation of DMIs. Instead, we found that populations evolved towards two regimes: either local adaptation and accumulation of DMIs with weak mate choice, or local adaptation with strict mate choice and no DMIs. This suggests two possible paths of speciation, one where ecological and genetic isolation dominate, and another where ecological and behavioral isolation dominate. The migration rate determined which regime was possible, with higher migration rates favoring the latter. It is thus not surprising that we recover results similar to the ones that have been derived for when two of the three RI mechanisms interact. This implies that under the genetic architecture with polygenic adaptation and multiple DMIs considered here, it is unlikely that populations evolve towards build up of strong pre- and post-zygotic barriers when there is gene flow. How loci involved in local adaptation and DMIs are distributed along the genome, and whether these different regimes lead to genetic signatures that can be detected based on polymorphism population genomics data remains to be further studied.

1 References

References

A. Agrawal, J. Feder, and P. Nosil. Ecological divergence and the origins of intrinsic postmating isolation with gene flow. *International Journal of Ecology*, 2011(1):435357, 2011.

S. Aguillon, S. K Haase Cox, Q. Langdon, T. Gunn, J. Baczenas, S. Banerjee, A. Donny, B. Moran, P. Fascinetto-Zago, C. Gutiérrez-Rodríguez, et al. Pervasive gene flow despite strong and varied reproductive barriers in swordtails. *Nature Ecology & Evolution*, pages 1–12, 2025.

J. Anderson, J. Funt, D. Thompson, S. Prabhu, A. Socha, C. Sirjusingh, J. Dettman, L. Parreiras, D. S Guttman, A. Regev, et al. Determinants of divergent adaptation and dobzhansky-muller interaction in experimental yeast populations. *Current Biology*, 20 (15):1383–1388, 2010.

S. Anderson and J. Weir. The role of divergent ecological adaptation during allopatric speciation in vertebrates. *Science*, 378(6625):1214–1218, 2022.

M. Andersson and Y. Iwasa. Sexual selection. *Trends in ecology & evolution*, 11(2):53–58, 1996.

T. Aubier, M. Kopp, I. Linn, O. Puebla, M. Rafajlović, and M. Servedio. Negative coupling: the coincidence of premating isolating barriers can reduce reproductive isolation. *Cold Spring Harbor Perspectives in Biology*, page a041435, 2024.

J. Ayala-López and C. Bank. What can we gain from modelling complex hybrid incompatibilities? *Evolutionary Journal of the Linnean Society*, 4(1):kzae034, 2025.

C. Bank, R. Bürger, and J. Hermisson. The limits to parapatric speciation: Dobzhansky–Muller incompatibilities in a continent–island model. *Genetics*, 191(3):845–863, 2012.

T. Barraclough. Does selection favour the maintenance of porous species boundaries? *Journal of Evolutionary Biology*, page voae030, 2024.

K. Barry and H. Kokko. Male mate choice: why sequential choice can make its evolution difficult. *Animal Behaviour*, 80(1):163–169, 2010.

N. Barton. Multilocus Clines. *Evolution*, 37(3):454, 1983.

W. Bateson. Heredity and variation in modern lights. *Darwin and modern science*, pages 85–101, 1909.

A. Blanckaert and J. Hermisson. The limits to parapatric speciation II: Strengthening a preexisting genetic barrier to gene flow in parapatry. *Genetics*, 209(1):241–254, 2018.

A. Blanckaert and B. Payseur. Finding hybrid incompatibilities using genome sequences from hybrid populations. *Molecular biology and evolution*, 38(10):4616–4627, 2021.

A. Blanckaert, C. Bank, and J. Hermisson. The limits to parapatric speciation 3: Evolution of strong reproductive isolation in presence of gene flow despite limited ecological differentiation. *Philosophical Transactions of the Royal Society of London. Series B, Biological Sciences*, 375(1806), 2020.

A. Blanckaert, V. Sriram, and C. Bank. In search of the goldilocks zone for hybrid speciation ii: hard times for hybrid speciation? *Evolution*, 77(10):2162–2172, 2023.

D. Bolnick, A. Hund, P. Nosil, F. Peng, M. Ravinet, S. Stankowski, S. Subramanian, J. Wolf, and R. Yukilevich. A multivariate view of the speciation continuum. *Evolution*, 77(1):318–328, 2023.

R. Butlin and C. Smadja. Coupling, reinforcement, and speciation. *The American Naturalist*, 191(2):155–172, 2018.

R. Butlin, J. Galindo, and J. Grahame. Sympatric, parapatric or allopatric: the most important way to classify speciation? *Philosophical Transactions of the Royal Society B: Biological Sciences*, 363(1506):2997–3007, 2008.

D. Castillo, M. Burger, C. Lively, and L. Delph. Experimental evolution: assortative mating and sexual selection, independent of local adaptation, lead to reproductive isolation in the nematode caenorhabditis remanei. *Evolution*, 69(12):3141–3155, 2015.

H. Chou, N. Delaney, J. Draghi, and C. Marx. Mapping the fitness landscape of gene expression uncovers the cause of antagonism and sign epistasis between adaptive mutations. *PLoS genetics*, 10(2):e1004149, 2014.

R. Corbett-Detig, J. Zhou, A. Clark, D. Hartl, and J. Ayroles. Genetic incompatibilities are widespread within species. *Nature*, 504(7478):135–137, 2013.

J. Coyne and H. Orr. *Speciation*. Sinauer Associates Sunderland, MA, 2004.

M. Cruz, S. Magalhães, M. Bakirdöven, and F. Zélé. Wolbachia strengthens the match between pre-mating and early post-mating isolation in spider mites. *bioRxiv*, pages 2024–05, 2024.

A. Cutter. The polymorphic prelude to Bateson–Dobzhansky–Muller incompatibilities. *Trends in ecology & evolution*, 27(4):209–218, 2012.

C. Darwin. *The origin of species*. London: Murray, 1859.

J. Dettman, C. Sirjusingh, L. Kohn, and J. Anderson. Incipient speciation by divergent adaptation and antagonistic epistasis in yeast. *Nature*, 447(7144):585–588, 2007.

J. Dettman, J. Anderson, and L. Kohn. Divergent adaptation promotes reproductive isolation among experimental populations of the filamentous fungus *Neurospora*. *BMC evolutionary biology*, 8(1):35, 2008.

T. Dobzhansky. Studies on hybrid sterility. II. Localization of sterility factors in *Drosophila pseudoobscura* hybrids. *Genetics*, 21(2):113, 1936.

E. Dopman, K. Shaw, M. Servedio, R. Butlin, and C. Smadja. Coupling of barriers to gene exchange: causes and consequences. *Cold Spring Harbor Perspectives in Biology*, page a041432, 2024.

M. Feldman, S. Otto, and F. Christiansen. Population genetic perspectives on the evolution of recombination. *Annual review of genetics*, 30(1):261–295, 1996.

R. A. Fisher. *The genetical theory of natural selection*. Oxford University Press, Oxford, 1930.

C. Fitzpatrick and M. Servedio. The evolution of male mate choice and female ornamentation: a review of mathematical models. *Current zoology*, 64(3):323–333, 2018.

M. Frayer, N. Robles, M. Barrera, J. Coughlan, and M. Schumer. The molecular evolutionary basis of species formation revisited. 2025.

C. Fraïsse, P. A. Gunnarsson, D. Roze, N. Bierne, and J. J. Welch. The genetics of speciation: Insights from fisher's geometric model. *Evolution*, 2016.

P. Grant and R. Grant. From microcosm to macrocosm: adaptive radiation of darwin's finches. *Evolutionary Journal of the Linnean Society*, 3(1):kzae006, 2024.

P.A. Gros, H. Le Nagard, and O. Tenaillon. The evolution of epistasis and its links with genetic robustness, complexity and drift in a phenotypic model of adaptation. *Genetics*, 182(1):277–293, 2009.

R. Guerrero, C. Muir, S. Josway, and L. Moyle. Pervasive antagonistic interactions among hybrid incompatibility loci. *PLoS Genetics*, 13(6):e1006817, 2017.

J. Haldane. The relative importance of principal and modifying genes in determining some human diseases. *Journal of Genetics*, 41:149–157, 1941.

T. Hatfield and D. Schluter. Ecological speciation in sticklebacks: environment-dependent hybrid fitness. *Evolution*, 53(3):866–873, 1999.

J. Hey and C. Pinho. Population genetics and objectivity in species diagnosis. *Evolution*, 66(5):1413–1429, 2012.

D. Irwin. Assortative mating in hybrid zones is remarkably ineffective in promoting speciation. *The American Naturalist*, 195(6):E150–E167, 2020.

P. Jay, M. Chouteau, A. Whibley, H. Bastide, H. Parrinello, V. Llaurens, and M. Joron. Mutation load at a mimicry supergene sheds new light on the evolution of inversion polymorphisms. *Nature genetics*, 53(3):288–293, 2021.

Y. Jiang, D. Bolnick, and M. Kirkpatrick. Assortative mating in animals. *The American Naturalist*, 181(6):E125–E138, 2013.

C. Jiggins, I. Emelianov, and J. Mallet. Assortative mating and speciation as pleiotropic effects of ecological adaptation: Examples in moths and butterflies. 2005.

C. D Jiggins, R. Naisbit, R. Coe, and J. Mallet. Reproductive isolation caused by colour pattern mimicry. *Nature*, 411(6835):302–305, 2001.

K. Johannesson, R. Faria, A. Le Moan, M. Rafajlović, A. Westram, R. Butlin, and S. Stankowski. Diverse pathways to speciation revealed by marine snails. *Trends in Genetics*, 40(4):337–351, 2024.

K. Kao, K. Schwartz, and G. Sherlock. A genome-wide analysis reveals no nuclear Dobzhansky-Muller pairs of determinants of speciation between S. cerevisiae and S. paradoxus, but suggests more complex incompatibilities. *PLoS genetics*, 6(7):e1001038, 2010.

M. Kirkpatrick and N. Barton. Chromosome inversions, local adaptation and speciation. *Genetics*, 173(1):419–434, 2006.

M. Kirkpatrick and V. Ravigné. Speciation by natural and sexual selection: models and experiments. *the american naturalist*, 159(S3):S22–S35, 2002.

J. Kitano and G. Okude. Causative genes of intrinsic hybrid incompatibility in animals and plants: what we have learned about speciation from the molecular perspective. *Evolutionary Journal of the Linnean Society*, 3(1):kzae022, 2024.

J. Kulmuni and A. Westram. Intrinsic incompatibilities evolving as a by-product of divergent ecological selection: Considering them in empirical studies on divergence with gene flow. *Molecular Ecology*, 26(12):3093–3103, 2017.

D. Kvitek and G. Sherlock. Reciprocal sign epistasis between frequently experimentally evolved adaptive mutations causes a rugged fitness landscape. *PLoS genetics*, 7(4): e1002056, 2011.

Y. Lee, C. Marsden, L. Norris, T. Collier, B. Main, A. Fofana, A. Cornel, and G. Lanzaro. Spatiotemporal dynamics of gene flow and hybrid fitness between the m and s forms of the malaria mosquito, anopheles gambiae. *Proceedings of the National Academy of Sciences*, 110(49):19854–19859, 2013.

T. Mackay. The genetic architecture of quantitative traits. *Annual review of genetics*, 35 (1):303–339, 2001.

M. Macnair and P. Christie. Reproductive isolation as a pleiotropic effect of copper tolerance in mimulus guttatus? *Heredity*, 50(3):295–302, 1983.

L. Maisonneuve, C. Smadi, and V. Llaurens. Which cues are sexy? the evolution of mate preference in sympatric species reveals the contrasted effect of adaptation and reproductive interference. *Evolution Letters*, 8(2):283–294, 2024.

J. Mallet and N. Barton. Strong natural selection in a warning-color hybrid zone. *Evolution*, 43(2):421–431, 1989.

J. Mallet and S. Mullen. Reproductive isolation is a heuristic, not a measure: a commentary on westram et al., 2022. *Journal of Evolutionary Biology*, 35(9):1175–1182, 2022.

D. Marques, K. Lucek, V. Sousa, L. Excoffier, and O. Seehausen. Admixture between old lineages facilitated contemporary ecological speciation in lake constance stickleback. *Nature communications*, 10(1):4240, 2019.

G. Martin and T. Lenormand. A general multivariate extension of fisher's geometrical model and the distribution of mutation fitness effects across species. *Evolution*, 60(5): 893–907, 2006.

M. McGee, S. Borstein, J. Meier, D. Marques, S. Mwaiko, A. Taabu, M. Kishe, B. O'Meara, R. Bruggmann, L. Excoffier, et al. The ecological and genomic basis of explosive adaptive radiation. *Nature*, 586(7827):75–79, 2020.

J. McKinnon, S. Mori, B. Blackman, L. David, D. Kingsley, L. Jamieson, J. Chou, and D. Schluter. Evidence for ecology's role in speciation. *Nature*, 429(6989):294–298, 2004.

M. McPeek and S. Gavrilets. The evolution of female mating preferences: differentiation from species with promiscuous males can promote speciation. *Evolution*, 60(10):1967–1980, 2006.

C. Mérot, E. Berdan, H. Cayuela, H. Djambazian, A. Ferchaud, M. Laporte, E. Normandeau, J. Ragoussis, M. Wellenreuther, and L. Bernatchez. Locally adaptive inversions modulate genetic variation at different geographic scales in a seaweed fly. *Molecular biology and evolution*, 38(9):3953–3971, 2021.

H. Muller. Isolating mechanisms, evolution and temperature. In *Biol. Symp*, volume 6, pages 71–125, 1942.

M. Nei. Modification of linkage intensity by natural selection. *Genetics*, 57(3):625, 1967.

P. Nosil. *Ecological speciation*. Oxford University Press, 2012.

P. Nouhaud, A. Blanckaert, C. Bank, and J. Kulmuni. Understanding admixture: haplodiploidy to the rescue. *Trends in Ecology & Evolution*, 35(1):34–42, 2020.

J. Ono, A. Gerstein, and S. Otto. Widespread Genetic Incompatibilities between First-Step Mutations during Parallel Adaptation of *Saccharomyces cerevisiae* to a Common Environment. *PLoS biology*, 15(1):e1002591, 2017.

H. Orr. The population genetics of speciation: the evolution of hybrid incompatibilities. *Genetics*, 139(4):1805–1813, 1995.

C. Payne, R. Bovio, D. Powell, T. Gunn, S. Banerjee, V. Grant, G. Rosenthal, and M. Schumer. Genomic insights into variation in thermotolerance between hybridizing swordtail fishes. *Molecular Ecology*, 33(23):e16489, 2024.

B. Payseur and L. Rieseberg. A genomic perspective on hybridization and speciation. *Molecular ecology*, 25(11):2337–2360, 2016.

A. Pomiankowski, Y. Iwasa, and S. Nee. The evolution of costly mate preferences i. fisher and biased mutation. *Evolution*, 45(6):1422–1430, 1991.

D. Powell, M. García-Olazábal, M. Keegan, P. Reilly, K. Du, A. Díaz-Loyo, S. Banerjee, D. Blakkan, D. Reich, P. Andolfatto, et al. Natural hybridization reveals incompatible alleles that cause melanoma in swordtail fish. *Science*, 368(6492):731–736, 2020.

D. Presgraves. A fine-scale genetic analysis of hybrid incompatibilities in *Drosophila*. *Genetics*, 163(3):955–972, 2003.

S. Rogers and L. Bernatchez. The genetic architecture of ecological speciation and the association with signatures of selection in natural lake whitefish (coregonus sp. salmonidae) species pairs. *Molecular biology and evolution*, 24(6):1423–1438, 2007.

H. Rundle and P. Nosil. Ecological speciation. *Ecology letters*, 8(3):336–352, 2005.

D. Schluter and G. Conte. Genetics and ecological speciation. *Proceedings of the National Academy of Sciences*, 106(supplement_1):9955–9962, 2009.

M. Servedio and J. Boughman. The role of sexual selection in local adaptation and speciation. *Annual Review of Ecology, Evolution, and Systematics*, 48(1):85–109, 2017.

M. Servedio and J. Hermisson. The evolution of partial reproductive isolation as an adaptive optimum. *Evolution*, 74(1):4–14, 2020.

M. Servedio, GS. Van Doorn, M. Kopp, A. Frame, and P. Nosil. Magic traits in speciation:'magic'but not rare? *Trends in ecology & evolution*, 26(8):389–397, 2011.

R. Snyder and H. Dingle. Adaptive, genetically based differences in life history between estuary and freshwater threespine sticklebacks (gasterosteus aculeatus l.). *Canadian Journal of Zoology*, 67(10):2448–2454, 1989.

J. Sobel, G. Chen, L. Watt, and D. Schemske. The biology of speciation. *Evolution*, 64 (2):295–315, 2010.

S. Stankowski and M. Ravinet. Defining the speciation continuum. *Evolution*, 75(6): 1256–1273, 2021.

F. Stearns and C. Fenster. Fisher's geometric model predicts the effects of random mutations when tested in the wild. *Evolution*, 70(2):495–501, 2016.

R. Stelkens, K. Young, and O. Seehausen. The accumulation of reproductive incompatibilities in african cichlid fish. *Evolution: International Journal of Organic Evolution*, 64(3):617–633, 2010.

R. Stelkens, C. Schmid, and O. Seehausen. Hybrid breakdown in cichlid fish. *PloS one*, 10(5):e0127207, 2015.

M. Świadek, S. Proost, D. Sieh, J. Yu, M. Todesco, C. Jorzig, A. Rodriguez Cubillos, B. Plötner, Z. Nikoloski, E. Chae, et al. Novel allelic variants in acd6 cause hybrid necrosis in local collection of arabidopsis thaliana. *New Phytologist*, 213(2):900–915, 2017.

X. Thibert-Plante and S. Gavrilets. Evolution of mate choice and the so-called magic traits in ecological speciation. *Ecology letters*, 16(8):1004–1013, 2013.

T. Turner, M. Hahn, and S. Nuzhdin. Genomic islands of speciation in anopheles gambiae. *PLoS Biol*, 3(9):e285, 2005.

S. Via, A. Bouck, and S. Skillman. Reproductive isolation between divergent races of pea aphids on two hosts. ii. selection against migrants and hybrids in the parental environments. *Evolution*, 54(5):1626–1637, 2000.

E. Villacis-Perez, F. De Graeve, B. De Beer, S. Ali Alshami, R. De Jong, T. De Meyer, and T. Van Leeuwen. Independent genetic mapping experiments identify diverse molecular determinants of host adaptation in a generalist herbivore. *Molecular Ecology*, page e17618, 2024.

B. Wallace. Polymorphism, population size, and genetic load. *Population biology and evolution*, pages 87–108, 1968.

B. Wallace. Hard and soft selection revisited. *Evolution*, pages 465–473, 1975.

A. Westram, S. Stankowski, P. Surendranadh, and N. Barton. What is reproductive isolation? *Journal of evolutionary biology*, 35(9):1143–1164, 2022.

R. Yamaguchi and Y. Iwasa. Reproductive character displacement by the evolution of female mate choice. *Evolutionary Ecology Research*, 15(1):25–41, 2013.